

Hierarchical Enumeration Based on Skeletons of Ligancy 6 by Using Combined-Permutation Representations. Part 1. Cyclopropane Derivatives

Shinsaku Fujita

Shonan Institute of Chemoinformatics and Mathematical Chemistry,

Kaneko 479-7 Ooimachi, Ashigara-Kami-Gun, Kanagawa-Ken,

258-0019 Japan

shinsaku.fujita@nifty.com

(Received April 4, 2017)

Abstract

Group hierarchy for characterizing a cyclopropane skeleton with six substitution positions has been discussed by defining the point group (PG), the *RS*-stereoisomeric group (*RS*-SIG), the stereoisomeric group (SIG), and the isoskeletal group (ISG) successively as follows: PG D_{3h} (order 12) \subset *RS*-SIG $D_{3h\bar{\sigma}\hat{I}}$ (order 24) \subset SIG $\tilde{D}_{3h\bar{\sigma}\hat{I}}$ (order 96) \subset ISG $\tilde{\tilde{D}}_{3h\bar{\sigma}\hat{I}}$ (order 1440). Combined-permutation representations, which have been originally developed for point groups and defined as the combination of permutation representations of groups and a mirror-permutation representation (S. Fujita, *MATCH Commun. Math. Comput. Chem.* **76** (2016) 379–400), are applied to the above group hierarchy. Then, according to Fujita's proligand method (S. Fujita, *Combinatorial Enumeration of Graphs, Three-Dimensional Structures, and Chemical Compounds*, University of Kragujevac, Faculty of Science, Kragujevac, 2013), enumerations of cyclopropane derivatives (as 3D structures) under PG and under *RS*-SIG are conducted by using cycle indices with chirality fittingness (CI-CFs) and a set of three ligand-inventory functions. On the other hand, enumerations of cyclopropane derivatives (as 2D structures or graphs) under SIG and under ISG are conducted by using a single ligand-inventory function, which implies the degeneration of CI-CFs into cycle indices without chirality fittingness (CIs). The enumeration results are discussed systematically in terms of isomer-classification diagrams.

1 Introduction

1.1 Unsettled interpretation on reflections

The term *reflection* is defined as an operation about a mirror plane, where the resulting mirror image is superposable on the original molecular entity (object). In the conventions of chemistry, physics, and mathematics, this term has been based on the presumption that any moiety of such a molecular entity (e.g., a ligand) can be regarded as a point which has no structure. This presumption has permitted the substitution of a permutation for a reflection, as found in the permutational approach by Ugi et al. [1]. This course has caused a serious confusion, because a rotation is also represented by a permutation. For example, Mislow and Siegel [2] stated “The symmetry of the labeled tetrahedron is a subgroup of T_d . Accordingly, the regular tetrahedron functions as a permutation center or skeleton with four equivalent sites, and models of stereoisomers are generated by permutation of the ligands among these sites.” This statement is seemingly rational if each sentence of this statement is focused independently. In spite of the word “Accordingly”, however, the second sentence of this statement cannot be deduced from the first sentence. Thus, this statement is totally found to be misleading because the point group T_d (with rotations and reflections) is considered to be characterized by a permutation group without differentiating reflections from rotations. In other words, the point group T_d is mixed up with the symmetric group of degree 4 ($S^{[4]}$) as a permutation group, so that the first sentence of this statement should be revised by substituting the symmetric group of degree 4 ($S^{[4]}$) for the point group T_d . Although this revision is capable of avoiding the misleadingness of the original statement, the revised statement indicates, in turn, that the effects of reflections due to the point group T_d are excluded from our domain of thinking.

The misleadingness due to the confusion between reflections (e.g., under T_d) and permutations (e.g., under $S^{[4]}$) is hidden so long as ligands are structureless. However, note that a tetrahedral molecule having $ABp\bar{p}$ (A and B: achiral ligands at 1- and 2-positions; as well as p and \bar{p} : chiral ligands at 3- and 4-positions which construct a pair of enantiomeric ligands in isolation) is fixed by a reflection (e.g., $(\overline{1})(2)(\overline{3\ 4})$) to behave as an achiral molecule. This achiral behavior due to a reflection (e.g., $(\overline{1})(2)(\overline{3\ 4})$) cannot be characterized by a permutation (e.g., $(1)(2)(3\ 4)$), because a permutation of any two ligands (e.g., p and \bar{p}) produces another tetrahedral molecule having $AB\bar{p}p$, which is achiral and different from (or diastereomeric to) the original molecule.

The confusion due to permutation groups without differentiating reflections from rotations has been wide-spread in mathematical fields as well as in chemical fields. For example, the dihedral group D_m (order $2m$) has $2m$ rotational symmetry operations for characterizing a m -gon as a 3-dimensional entity, where the half are recognized to be m rotations about the axis perpendicular to the m -gon, while the other half are recognized to be m rotations through π about the two-fold axes lying in the plane of the m -gon (cf. Chapter 4 of [3]). However, the mathematical convention for characterizing the dihedral group D_m has permitted the usage of the 2-dimensional terms “rotations about the center” and “reflections in the diameters” (page 143 of [4]), where the latter term “reflections in the diameters” of the m -gon is allowed in place of rotations through π (in 3-dimensional space) about the two-fold axes (the diameters).

This convention has been further transmuted into the definition of the “dihedral group” in several textbooks (e.g., page 20 of [5]) and in Wikipedia [6], where the dihedral group D_m is defined as the group of symmetries of a regular polygons, which includes rotations and reflections. The transmutation of the term “reflection” stems from the presumption that both reflections and rotations are represented by permutations. As a result, the dihedral group D_m cannot be differentiated from the point group C_{mv} used in chemistry. Hence, this transmuted usage of term “reflections” in the mathematical convention should be avoided. Instead, “reflections in the diameters” and “rotations through π about the diameters” should be strictly discriminated as found in a recent article [7], where both of them are considered to be 3D-based concepts in the α, β -itemized enumeration of inositol derivatives and m -gonal homologs.

1.2 Sphericities and stereoisograms for rationalizing the effects of reflections

The effects of reflections on ligands having 3D structures have been rationally evaluated by the concept of *sphericities of orbits* (homospheric, enantiospheric, and hemispheric orbits), which has been proposed by the author (Fujita) [8]. The sphericity of each orbit controls the *chirality fittingness* (CF) of the orbit, which determines the substitution modes of ligands having 3D structures, either chiral or achiral in isolation. The concepts of sphericities and chirality fittingness have been combined with the concept of *subduction of coset representations* so as to give the concepts of unit subduced cycle indices without and with chirality fittingness (USCIs and USCIs-CFs). These concepts have given the-

oretical foundations to the four methods of symmetry-itemized enumeration of organic compounds. The approach based on USCIs and USCI-CFs are collectively referred to as the USCI (unit-subduced-cycle-index) approach [9,10].

The concept of *sphericities of orbits* for Fujita's USCI approach has been transformed into the concept of *sphericities of cycles* (homospheric, enantiospheric, and hemispheric cycles) [11–13], which has alternatively enabled us to evaluate the effects of reflections on ligands having 3D structures. The resulting concepts of cycle indices without and with chirality fittingness (CIs and CI-CFs) have provided the theoretical foundation of the proligand method for gross-enumeration of organic compounds [14]. Fujita's proligand method and related methods for gross-enumeration have been comprehensively applied to the enumeration of cubane derivatives, as reported in this journal [15–19].

For the purpose of comprehending reflections and permutations, the author (Fujita) has proposed the stereoisogram approach [20], where permutations are restricted to *RS*-permutations, so as to clarify the net interaction with reflections [21,22]. Then, rotations, reflections, and *RS*-permutations are integrated to create an *RS*-stereoisomeric group, where the concepts of holantimers and ligand-reflections are proposed as missing links for integration. Such an *RS*-stereoisomeric group is diagrammatically represented by a stereoisogram, which consists of a quadruplet of *RS*-stereoisomers, i.e., a reference entity corresponding to rotations, an enantiomer corresponding to reflections, an *RS*-diastereomer corresponding to *RS*-permutations, and a holantimer corresponding to ligand-reflections.

1.3 Combined-permutation representations for computer manipulation of reflections

A reflection is represented by a permutation with an overbar (e.g., $\overline{(1)(2)(3\ 4)}$) in Fujita's USCI approach [9,10], Fujita's proligand method [14], and Fujita's stereoisogram approach [20], where the overbar indicates that a chiral ligand is converted into the enantiomeric ligand (in isolation). However, this type of representations are unsuitable for practical computer-manipulation.

It is highly desirable to develop a new representation suitable for practical calculations by computer systems such as the GAP (Groups, Algorithms, Programming) system [23]. Combined-permutation representations (CPRs) have recently been developed by the author (Fujita) as computer-oriented representations of point groups, where an overbar of

a reflection (e.g., $\overline{(1)(2)(3\ 4)}$) is replaced by an additional 2-cycle (e.g., (5 6)) to give a combined permutation (e.g., (1)(2)(3 4)(5 6)). The CPRs of the point group \mathbf{T}_d and related groups have been applied to gross enumeration of 3D structures of ligancy 4 [24]. The CPRs of the point group \mathbf{O}_h have been applied to gross enumeration of octahedral and cubane derivatives [25].

1.4 Aims of the present article

The CPRs for point groups have been extended to cover *RS*-stereoisomeric groups [26]. The next task is the systematic examination of the group hierarchy represented generally by the following scheme:

$$\begin{aligned} \text{point groups (PG)} &\subseteq \textit{RS}\text{-stereoisomeric groups (RS-SIG)} \\ &\subseteq \text{stereoisomeric groups (SIG)} \subseteq \text{isoskeletal groups (ISG)}. \end{aligned} \quad (1)$$

Because each symbol \subseteq can be altered to represent a net subset (\subset) or an equality ($=$) in accord with a skeleton to be examined, the mode of such alternation should be investigated systematically. The present article is devoted to the further extension of CPRs to cover hierarchy of isomer classification by using a cyclopropane skeleton as a probe for skeletons of ligancy 6.

2 Hierarchy of groups for characterizing a cyclopropane skeleton

The group hierarchy for characterizing a cyclopropane skeleton of ligancy 6 is partly shown in Figure 1, where the point group (PG) \mathbf{D}_{3h} (order 12) for enantiomerism, the *RS*-stereoisomeric group (*RS*-SIG) $\mathbf{D}_{3h\bar{\sigma}\hat{\Gamma}}$ (order 24) for *RS*-stereoisomerism, and the stereoisomeric group (SIG) $\tilde{\mathbf{D}}_{3h\bar{\sigma}\hat{\Gamma}}$ (order 96) for stereoisomerism are listed in a nested fashion. By adding the isoskeletal group (ISG) $\tilde{\tilde{\mathbf{D}}}_{3h\bar{\sigma}\hat{\Gamma}}$ (order 1440), the total group hierarchy for the cyclopropane skeleton is represented by the following scheme:

$$\text{PG } \mathbf{D}_{3h} \subset \textit{RS}\text{-SIG } \mathbf{D}_{3h\bar{\sigma}\hat{\Gamma}} \subset \text{SIG } \tilde{\mathbf{D}}_{3h\bar{\sigma}\hat{\Gamma}} \subset \text{ISG } \tilde{\tilde{\mathbf{D}}}_{3h\bar{\sigma}\hat{\Gamma}}, \quad (2)$$

which contains no equality symbols in contrast to the general scheme (Eq. 1).

Stereoisomeric group $\widetilde{D}_{3h\widehat{\sigma}\widehat{\tau}} = D_{3h\widehat{\sigma}\widehat{\tau}} + D_{3h\widehat{\sigma}\widehat{\tau}}\overline{\sigma}_{11} + D_{3h\widehat{\sigma}\widehat{\tau}}\overline{\sigma}_{25} + D_{3h\widehat{\sigma}\widehat{\tau}}\overline{\sigma}_{36}$			
RS -Stereoisomeric group $D_{3h\widehat{\sigma}\widehat{\tau}}$		$D_{3h\widehat{\sigma}\widehat{\tau}}\overline{\sigma}_{11}$	
	1		2
D_3	I (1)(2)(3)(4)(5)(6) h_1^6 C_3 (1 2 3)(4 5 6) h_2^3 C_2^3 (1 3 2)(4 6 5) h_3^2 $C_{2(1)}$ (1 4)(2 6)(3 5) h_4^2 $C_{2(2)}$ (1 6)(2 5)(3 4) h_5^2 $C_{2(3)}$ (1 5)(2 4)(3 6) h_6^2	D_{3h}	$\overline{\sigma}_6$ (1)(2)(3)(4)(5)(6) h_1^6 \overline{S}_3 (1 5 3 4 2 6) h_2^3 \overline{S}_2^3 (1 6 2 4 3 5) h_3^2 $\overline{\sigma}_{(1)}$ (1)(2 3)(4)(5 6) h_4^2 $\overline{\sigma}_{(2)}$ (1 3)(2)(4 6)(5) h_5^2 $\overline{\sigma}_{(3)}$ (1 2)(3)(4 5)(6) h_6^2
	3		4
D_{3h}	$I\overline{\sigma}_{11}$ (1 4)(2)(3)(5)(6) h_1^6 $C_3\overline{\sigma}_{11}$ (1 2 3 4 5 6) h_2^3 $C_2^3\overline{\sigma}_{11}$ (1 3 2 4 6 5) h_3^2 $C_{2(1)}\overline{\sigma}_{11}$ (1)(2 6)(3 5)(4) h_4^2 $C_{2(2)}\overline{\sigma}_{11}$ (1 6 4 3)(2 5) h_5^2 $C_{2(3)}\overline{\sigma}_{11}$ (1 5 4 2)(3 6) h_6^2	$D_{3h}\overline{\sigma}_{11}$	$\overline{\sigma}_6\overline{\sigma}_{11}$ (1)(2 5)(3 6)(4) h_1^6 $\overline{S}_3\overline{\sigma}_{11}$ (1 2 3 4 5 6) h_2^3 $\overline{S}_2^3\overline{\sigma}_{11}$ (1 6 2)(3 5 4) h_3^2 $\overline{\sigma}_{(1)}\overline{\sigma}_{11}$ (1 4)(2 3)(5 6) h_4^2 $\overline{\sigma}_{(2)}\overline{\sigma}_{11}$ (1 6 4 3)(2 5) h_5^2 $\overline{\sigma}_{(3)}\overline{\sigma}_{11}$ (1 2 4 5)(3 6) h_6^2
	5		6
D_{3h}	$I\overline{\sigma}_{25}$ (1 4)(2 5)(3 6) h_1^6 S_6 (1 5 3 4 2 6) h_2^3 S_2^3 (1 6 2 4 3 5) h_3^2 $\overline{\sigma}_{(1)}$ (1)(2 3)(4)(5 6) h_4^2 $\overline{\sigma}_{(2)}$ (1 3)(2)(4 6)(5) h_5^2 $\overline{\sigma}_{(3)}$ (1 2)(3)(4 5)(6) h_6^2	$D_{3h}\overline{\sigma}_{25}$	$\overline{\sigma}_6\overline{\sigma}_{25}$ (1 4)(2)(3 6)(5) h_1^6 $\overline{S}_3\overline{\sigma}_{25}$ (1 2 6)(3 4 5) h_2^3 $\overline{S}_2^3\overline{\sigma}_{25}$ (1 6 5)(2 4 3) h_3^2 $\overline{\sigma}_{(1)}\overline{\sigma}_{25}$ (1)(2 3 5 6)(4) h_4^2 $\overline{\sigma}_{(2)}\overline{\sigma}_{25}$ (1 3 4 6)(2 5) h_5^2 $\overline{\sigma}_{(3)}\overline{\sigma}_{25}$ (1 5 4 2)(3 6) h_6^2
	7		8
D_{3h}	$I\overline{\sigma}_{36}$ (1 4)(2 3 6)(4 5) h_1^6 $C_3\overline{\sigma}_{36}$ (1 2 6 4 5 3) h_2^3 $C_2^3\overline{\sigma}_{36}$ (1 6 5 4 3 2) h_3^2 $C_{2(1)}\overline{\sigma}_{36}$ (1 4)(2 3 5 6) h_4^2 $C_{2(2)}\overline{\sigma}_{36}$ (1 3 4 6)(2 5) h_5^2 $C_{2(3)}\overline{\sigma}_{36}$ (1 5 4 2)(3 6) h_6^2	$D_{3h}\overline{\sigma}_{36}$	$\overline{\sigma}_6\overline{\sigma}_{36}$ (1 4)(2 5)(3 6) h_1^6 $\overline{S}_3\overline{\sigma}_{36}$ (1 5 6)(2 3 4) h_2^3 $\overline{S}_2^3\overline{\sigma}_{36}$ (1 3 5 4 2 6) h_3^2 $\overline{\sigma}_{(1)}\overline{\sigma}_{36}$ (1)(2 6 5 3)(4) h_4^2 $\overline{\sigma}_{(2)}\overline{\sigma}_{36}$ (1 6 4 3)(2 5) h_5^2 $\overline{\sigma}_{(3)}\overline{\sigma}_{36}$ (1 2)(3 6 4 5) h_6^2
	9		10
D_{3h}	$I\overline{\sigma}_{25}$ (1 4)(2 5)(3 6)(4) h_1^6 $S_6\overline{\sigma}_{25}$ (1 2 6)(3 4 5) h_2^3 $S_2^3\overline{\sigma}_{25}$ (1 6 5)(2 4 3) h_3^2 $\overline{\sigma}_{(1)}\overline{\sigma}_{25}$ (1)(2 3 5 6)(4) h_4^2 $\overline{\sigma}_{(2)}\overline{\sigma}_{25}$ (1 3)(2 5)(4 6) h_5^2 $\overline{\sigma}_{(3)}\overline{\sigma}_{25}$ (1 5 4 2)(3 6) h_6^2	$D_{3h}\overline{\sigma}_{25}$	$\overline{\sigma}_6\overline{\sigma}_{25}$ (1 4)(2 5)(3 6) h_1^6 $\overline{S}_3\overline{\sigma}_{25}$ (1 5 6 4 2 3) h_2^3 $\overline{S}_2^3\overline{\sigma}_{25}$ (1 3 5 4 6 2) h_3^2 $\overline{\sigma}_{(1)}\overline{\sigma}_{25}$ (1 4)(2 3 5 6)(4) h_4^2 $\overline{\sigma}_{(2)}\overline{\sigma}_{25}$ (1 6 4 3)(2 5) h_5^2 $\overline{\sigma}_{(3)}\overline{\sigma}_{25}$ (1 2 4 5)(3 6) h_6^2

Figure 1. RS -Stereoisomeric group $D_{3h\widehat{\sigma}\widehat{\tau}}$ and stereoisomeric group $\widetilde{D}_{3h\widehat{\sigma}\widehat{\tau}}$, which are derived from a coset representation of D_{3h} for characterizing cyclopropane derivatives. The product of sphericity indices (PSI) is attached to each element.

2.1 Point group D_{3h} for enantiomerism

The reference skeleton 1, is converted into homomeric skeletons under the action of the chiral point group D_3 listed in Figure 1. Note that the chiral point group D_3 , which is isomorphic to the dihedral group D_3 of degree 3 (order 6), is considered to contain rotations and no reflections, as discussed in Introduction (cf. Subsection 1.1). The point group D_{3h} is

constructed as follows:

$$\mathbf{D}_{3h} = \mathbf{D}_3 + \mathbf{D}_3\sigma_h, \quad (3)$$

where the symbol σ_h represents a reflection about a cyclopropane ring as a mirror plane ($\sigma_h \sim \overline{(1\ 4)(2\ 5)(3\ 6)}$). The action of each element contained in the coset $\mathbf{D}_3\sigma_h$ on the reference skeleton **1** generates the corresponding mirror-numbered skeleton $\bar{\mathbf{1}}$ or its homomer.

2.2 *RS*-stereoisomeric group $\mathbf{D}_{3h\tilde{\sigma}\hat{I}}$ for *RS*-stereoisomerism

Let us define an *RS*-permutation $\tilde{\sigma}_h$ as an operation which is generated by omitting ligand reflections from the reflection σ_h , i.e., $\tilde{\sigma}_h \sim (1\ 4)(2\ 5)(3\ 6)$. Then, the *RS*-permutation group $\mathbf{D}_{3\tilde{\sigma}}$ is constructed as follows:

$$\mathbf{D}_{3\tilde{\sigma}} = \mathbf{D}_3 + \mathbf{D}_3\tilde{\sigma}_h. \quad (4)$$

The action of each element contained in the coset $\mathbf{D}_3\tilde{\sigma}_h$ on the reference skeleton **1** generates the corresponding *RS*-numbered skeleton **2** or its homomer. Note that the *RS*-numbered skeleton **2** is *RS*-diastereomeric to the reference skeleton **1**.

Let us next define a ligand-reflection \hat{I} as an operation which is generated by adding ligand reflections to an identity operation I , i.e., $\hat{I} \sim \overline{(1)(2)(3)(4)(5)(6)}$. Then, the ligand-reflection group $\mathbf{D}_{3\hat{I}}$ is constructed as follows:

$$\mathbf{D}_{3\hat{I}} = \mathbf{D}_3 + \mathbf{D}_3\hat{I}. \quad (5)$$

The action of each element contained in the coset $\mathbf{D}_3\hat{I}$ on the reference skeleton **1** generates the corresponding *LR*-numbered skeleton $\bar{\mathbf{2}}$ or its homomer. Note that the *LR*-numbered skeleton $\bar{\mathbf{2}}$ is halantimeric to the reference skeleton **1** and that it is enantiomeric to the *RS*-numbered skeleton **2**.

Because the point group \mathbf{D}_3 is contained commonly in \mathbf{D}_{3h} (Eq. 3), $\mathbf{D}_{3\tilde{\sigma}}$ (Eq. 4), and $\mathbf{D}_{3\hat{I}}$ (Eq. 5), these groups are integrated into the following *RS*-stereoisomeric group:

$$\mathbf{D}_{3h\tilde{\sigma}\hat{I}} = \mathbf{D}_3 + \mathbf{D}_3\sigma_h + \mathbf{D}_3\tilde{\sigma}_h + \mathbf{D}_3\hat{I}, \quad (6)$$

the 24 elements of which are listed in the upper-left part of Figure 1. The corresponding quadruplet of *RS*-stereoisomeric skeletons (**1** for the coset \mathbf{D}_3I , $\bar{\mathbf{1}}$ for the coset $\mathbf{D}_3\sigma_h$, **2** for the coset $\mathbf{D}_3\tilde{\sigma}_h$, and $\bar{\mathbf{2}}$ for the coset $\mathbf{D}_3\hat{I}$) is capable of constructing a stereoisogram

by placing ligands (or proligands in an abstract fashion) on the six substitution positions. The order $|\mathbf{D}_{3h\tilde{\sigma}\hat{I}}|$ is calculated to be 24 ($= |\mathbf{D}_3| \times 4 = 6 \times 4$) by referring to Eq. 6.

Because of Eq. 3 for point group \mathbf{D}_{3h} , the RS -stereoisomeric group $\mathbf{D}_{3h\tilde{\sigma}\hat{I}}$ (Eq. 6) is also generated by the following coset decomposition:

$$\mathbf{D}_{3h\tilde{\sigma}\hat{I}} = \mathbf{D}_{3h} + \mathbf{D}_{3h}\tilde{\sigma}_h, \quad (7)$$

where we use $\sigma_h\tilde{\sigma}_h = \hat{I}$ during the calculation of the second coset, i.e., $\mathbf{D}_3\tilde{\sigma}_h + \mathbf{D}_3\hat{I} = (\mathbf{D}_3 + \mathbf{D}_3\sigma_h)\tilde{\sigma}_h = \mathbf{D}_{3h}\tilde{\sigma}_h$.

2.3 Stereoisomeric group $\tilde{\mathbf{D}}_{3h\tilde{\sigma}\hat{I}}$ for stereoisomerism

For the purpose of discussing stereoisomerism, we consider three epimerization operations designated by the symbols $\tilde{\sigma}_{14}$, $\tilde{\sigma}_{25}$, and $\tilde{\sigma}_{36}$, which correspond to permutations (1 4)(2)(3)(5)(6), (1)(2 5)(3)(4)(6), and (1)(2)(3 4)(5)(6), respectively. These epimerization operations are not accompanied with ligand reflections, so as to give the respective numbered skeletons **3**, **5**, and **7**. Thereby, the stereoisomeric group $\tilde{\mathbf{D}}_{3h\tilde{\sigma}\hat{I}}$ (order 96) is constructed by the following coset decomposition:

$$\tilde{\mathbf{D}}_{3h\tilde{\sigma}\hat{I}} = \mathbf{D}_{3h\tilde{\sigma}\hat{I}} + \mathbf{D}_{3h\tilde{\sigma}\hat{I}}\tilde{\sigma}_{14} + \mathbf{D}_{3h\tilde{\sigma}\hat{I}}\tilde{\sigma}_{25} + \mathbf{D}_{3h\tilde{\sigma}\hat{I}}\tilde{\sigma}_{36}. \quad (8)$$

The elements of the respective cosets are listed in the respective parts of Figure 1. The order $|\tilde{\mathbf{D}}_{3h\tilde{\sigma}\hat{I}}|$ is calculated to be 96 ($= |\mathbf{D}_{3h\tilde{\sigma}\hat{I}}| \times 4 = 24 \times 4$) by referring to Eq. 8.

2.4 Isoskeletal group $\tilde{\tilde{\mathbf{D}}}_{3h\tilde{\sigma}\hat{I}}$ for isoskeletomerism

The isoskeletal group $\tilde{\tilde{\mathbf{D}}}_{3h\tilde{\sigma}\hat{I}}$ (order 1440) is introduced to characterize the isoskeletomerism of a cyclopropane skeleton **1**, where we consider 14 isoskeletal operations, i.e.,

$$\begin{aligned} \tilde{\sigma}_{56} &\sim (1)(2)(3)(4)(5\ 6), & \tilde{\sigma}_{45} &\sim (1)(2)(3)(4\ 5)(6), & \tilde{\sigma}_{456} &\sim (1)(2)(3)(4\ 5\ 6), \\ \tilde{\sigma}_{465} &\sim (1)(2)(3)(4\ 6\ 5), & \tilde{\sigma}_{46} &\sim (1)(2)(3)(4\ 6)(5), & \tilde{\sigma}_{34} &\sim (1)(2)(3\ 4)(5)(6), \\ \tilde{\sigma}_{34,56} &\sim (1)(2)(3\ 4)(5\ 6), & \tilde{\sigma}_{345} &\sim (1)(2)(3\ 4\ 5)(6), & \tilde{\sigma}_{3465} &\sim (1)(2)(3\ 4\ 6\ 5), \\ \tilde{\sigma}_{354} &\sim (1)(2)(3\ 5\ 4)(6), & \tilde{\sigma}_{35} &\sim (1)(2)(3\ 5)(4)(6), & \tilde{\sigma}_{234} &\sim (1)(2\ 3\ 4)(5)(6), \\ \tilde{\sigma}_{234,56} &\sim (1)(2\ 3\ 4)(5\ 6), & \tilde{\sigma}_{2354} &\sim (1)(2\ 3\ 5\ 4)(6). \end{aligned} \quad (9)$$

These isoskeletal operations (in addition to an identity operation) are regarded as transversals to construct the following coset decomposition:

$$\tilde{\tilde{\mathbf{D}}}_{3h\tilde{\sigma}\hat{I}} = \tilde{\mathbf{D}}_{3h\tilde{\sigma}\hat{I}} + \tilde{\mathbf{D}}_{3h\tilde{\sigma}\hat{I}}\tilde{\sigma}_{56} + \tilde{\mathbf{D}}_{3h\tilde{\sigma}\hat{I}}\tilde{\sigma}_{45} + \tilde{\mathbf{D}}_{3h\tilde{\sigma}\hat{I}}\tilde{\sigma}_{456} + \tilde{\mathbf{D}}_{3h\tilde{\sigma}\hat{I}}\tilde{\sigma}_{465} +$$

$$\begin{aligned} & \tilde{D}_{3h\tilde{\sigma}\tilde{\Gamma}}\tilde{\sigma}_{46} + \tilde{D}_{3h\tilde{\sigma}\tilde{\Gamma}}\tilde{\sigma}_{34} + \tilde{D}_{3h\tilde{\sigma}\tilde{\Gamma}}\tilde{\sigma}_{34,56} + \tilde{D}_{3h\tilde{\sigma}\tilde{\Gamma}}\tilde{\sigma}_{345} + \tilde{D}_{3h\tilde{\sigma}\tilde{\Gamma}}\tilde{\sigma}_{3465} + \\ & \tilde{D}_{3h\tilde{\sigma}\tilde{\Gamma}}\tilde{\sigma}_{354} + \tilde{D}_{3h\tilde{\sigma}\tilde{\Gamma}}\tilde{\sigma}_{35} + \tilde{D}_{3h\tilde{\sigma}\tilde{\Gamma}}\tilde{\sigma}_{234} + \tilde{D}_{3h\tilde{\sigma}\tilde{\Gamma}}\tilde{\sigma}_{234,56} + \tilde{D}_{3h\tilde{\sigma}\tilde{\Gamma}}\tilde{\sigma}_{2354}, \end{aligned} \quad (10)$$

which designates the generation of the isoskeletal group $\tilde{D}_{3h\tilde{\sigma}\tilde{\Gamma}}$ for characterizing the isoskeletomerism of a cyclopropane skeleton **1**. The order $|\tilde{D}_{3h\tilde{\sigma}\tilde{\Gamma}}|$ is calculated to be 1440 ($= |\tilde{D}_{3h\tilde{\sigma}\tilde{\Gamma}}| \times 15 = 96 \times 15$) by referring to Eq. 10.

3 Combined representations

3.1 Coset representation for the point group D_{3h} and and the construction of its combined representation

The six positions of a cyclopropane skeleton **1** are regarded as constructing the following set:

$$\mathbf{X} = \{1, 2, 3, 4, 5, 6\}. \quad (11)$$

The action of the point group D_{3h} on the set \mathbf{X} is represented by a right-coset representation $(C_s \setminus)D_{3h}$, which is expressed in terms of products of cycles listed in the D_3 part and the $D_3\sigma_h$ part of Figure 1, e.g., $C_3 \sim (1\ 2\ 3)(4\ 5\ 6)$ for a 3-fold rotation and $\sigma_h \sim \overline{(1\ 4)(2\ 5)(3\ 6)}$ for a horizontal reflection. The GAP system adopts right-coset representations as standards and presumes that the multiplication of permutations is executed from left to right, so that the right-coset representation $(C_s \setminus)D_{3h}$ is adopted here in place of the corresponding left-coset representation $D_{3h}/(C_s)$.

The expressions with an overline for characterizing reflections are not suitable to treat such right-coset representations systematically by computer. Hence, the combined-permutation representation proposed by the author [24–26] is adopted for the purpose of systematic treatment by computer. The combined-permutation representation $P_{D_{3h}}^{(x,x)}$ (D3h) is obtained by combining the coset representation $(C_s \setminus)D_{3h}$ (or $D_{3h}/(C_s)$) with a mirror-permutation representation, which acts on the domain $\chi = \{7, 8\}$ to indicate a mirror permutation corresponding to an overline. Thereby, the respective elements contained in the $D_3\sigma_h$ -part of Figure 1 are represented as follows:

elements	$D_3\sigma_h$ part		
	$(C_s \setminus) D_{3h}$	$P_{D_{3h}}^{(xx)}$	D3h
σ_h	$(1\ 4)(2\ 5)(3\ 6)$	(1 4)(2 5)(3 6)(7 8)	(1, 4)(2, 5)(3, 6)(7, 8)
S_3	$(1\ 5\ 3\ 4\ 2\ 6)$	(1 5 3 4 2 6)(7 8)	(1, 5, 3, 4, 2, 6)(7, 8)
S_3^2	$(1\ 6\ 2\ 4\ 3\ 5)$	(1 6 2 4 3 5)(7 8)	(1, 6, 2, 4, 3, 5)(7, 8)
$\sigma_{v(1)}$	$(1)(2\ 3)(4)(5\ 6)$	(1)(2 3)(4)(5 6)(7 8)	(2, 3)(5, 6)(7, 8)
$\sigma_{v(2)}$	$(1\ 3)(2)(4\ 6)(5)$	(1 3)(2)(4 6)(5)(7 8)	(1, 3)(4, 6)(7, 8)
$\sigma_{v(3)}$	$(1\ 2)(3)(4\ 5)(6)$	(1 2)(3)(4 5)(6)(7 8)	(1, 2)(4, 5)(7, 8)

(12)

The last D3h-column of Eq. 12 lists concrete expressions used during the execution of the GAP system, where 1-cycles in $P_{D_{3h}}^{(xx)}$ are omitted and commas are added.

Because a combined-permutation representation (e.g., $P_{D_{3h}}^{(xx)}$ (D3h)) is used as a permutation group with an additional 2-cycle, we are able to reveal the group-theoretical properties of the original point group (e.g., D_{3h}) by computer (through the GAP system).

The D_{3h} -part of Table 1 collects the GAP codes for generating the combined representation D3h according to Eq. 3. The symbol `gap>` represents the prompt of the GAP system in the command-prompt window of the Windows system. Thus, the elements of the coset $D_3\sigma_h$ are obtained by the GAP code `e1m_D3*(1,4)(2,5)(3,6)(7,8)`, where the symbol `e1m_D3` represents a GAP list for the set of elements of D_3 (cf. the D_{3h} -part of Table 1). By using the GAP function `Concatenation`, the set of the elements of D_{3h} is obtained in the form of a GAP list named `e1m_D3h`. The resulting list `e1m_D3h` is consistent with the data collected in the D_{3h} -part of Figure 1. The list `e1m_D3h` can be transformed into a group D3h by using the GAP function `AsGroup`. The resulting group D3h is specified by the GAP function `Group` containing the generators of constructing the group D3h. Thereby, the combined representation D3h is regarded as a permutation group. The elements (`Elements(D3h)`) of the group D3h are identical with those of the list `e1m_D3h`, as confirmed by the GAP function `IsEqualSet`.

Table 1. Group Hierarchy for Characterizing a Cyclopropane Skeleton (Part 1)

group	list of elements for constructing a group
D_3 (point group) order: 6	<pre> gap> #Point group D3;; gap> elm_D3 := [(), (1,2,3)(4,5,6), (1,3,2)(4,6,5), (1,4)(2,6)(3,5), ↪ (1,6)(2,5)(3,4), (1,5)(2,4)(3,6)]; [(), (1,2,3)(4,5,6), (1,3,2)(4,6,5), (1,4)(2,6)(3,5), (1,6)(2,5)(3,4), (1,5)(2,4)(3,6)] gap> D3 := AsGroup(elm_D3); Group([(1,2,3)(4,5,6), (1,4)(2,6)(3,5)]) gap> Print("IsEqualSet(elm_D3,␣Elements(D3))␣?:␣", IsEqualSet(elm_D3, ↪ Elements(D3)), "\n"); IsEqualSet(elm_D3, Elements(D3)) ? : true gap> Print("Order␣of␣D3:␣", Size(D3), "\n"); Order of D3: 6 </pre>
D_{3h} (point group) order: 12	<pre> gap> #Point group D3h;; gap> elm_D3h := Concatenation(elm_D3, elm_D3*(1,4)(2,5)(3,6)(7,8)); [(), (1,2,3)(4,5,6), (1,3,2)(4,6,5), (1,4)(2,6)(3,5), (1,6)(2,5)(3,4), (1,5)(2,4)(3,6), (1,4)(2,5)(3,6)(7,8), (1,5,3,4,2,6)(7,8), (1,6,2,4,3,5)(7,8), (2,3)(5,6)(7,8), (1,3)(4,6)(7,8), (1,2)(4,5)(7,8)] gap> D3h := AsGroup(elm_D3h); Group([(2,3)(5,6)(7,8), (1,2)(4,5)(7,8), (1,4)(2,5)(3,6)(7,8)]) gap> Print("IsEqualSet(elm_D3h,␣Elements(D3h))␣?:␣", IsEqualSet(↪ elm_D3h, Elements(D3h)), "\n"); IsEqualSet(elm_D3h, Elements(D3h)) ? : true gap> Print("Order␣of␣D3h:␣", Size(D3h), "\n"); Order of D3h: 12 </pre>
$D_{3h\tilde{\sigma}\tilde{I}}$ (<i>RS</i> -stereo- isomeric group) order: 24	<pre> gap> #RS-stereoisomeric group;; gap> elm_D3hsI := Concatenation(elm_D3h, elm_D3h*(1,4)(2,5)(3,6)); [(), (1,2,3)(4,5,6), (1,3,2)(4,6,5), (1,4)(2,6)(3,5), (1,6)(2,5)(3,4), (1,5)(2,4)(3,6), (1,4)(2,5)(3,6)(7,8), (1,5,3,4,2,6)(7,8), (1,6,2,4,3,5)(7,8), (2,3)(5,6)(7,8), (1,3)(4,6)(7,8), (1,2)(4,5)(7,8), (1,4)(2,5)(3,6), (1,5,3,4,2,6), (1,6,2,4,3,5), (2,3)(5,6), (1,3)(4,6), (1,2)(4,5), (7,8), (1,2,3)(4,5,6)(7,8), (1,3,2)(4,6,5)(7,8), (1,4)(2,6)(3,5)(7,8), (1,6)(2,5)(3,4)(7,8), (1,5)(2,4)(3,6)(7,8)] gap> D3hsI := AsGroup(elm_D3hsI); Group([(7,8), (2,3)(5,6), (1,2)(4,5), (1,4)(2,5)(3,6)]) gap> Print("IsEqualSet(elm_D3hsI,␣Elements(D3hsI))␣?:␣", IsEqualSet(↪ elm_D3hsI, Elements(D3hsI)), "\n"); IsEqualSet(elm_D3hsI, Elements(D3hsI)) ? : true gap> Print("Order␣of␣D3hsI:␣", Size(D3hsI), "\n"); Order of D3hsI: 24 </pre>

3.2 Hierarchical calculation of combined representations

3.2.1 Combined representation $D_{3h\tilde{\sigma}\tilde{I}}$ for the *RS*-stereoisomeric group $D_{3h\tilde{\sigma}\tilde{I}}$

The $D_{3h\tilde{\sigma}\tilde{I}}$ -part of Table 1 collects the GAP codes for generating the combined representation $D_{3h\tilde{\sigma}\tilde{I}}$ according to Eq. 7. Thus, the elements of the coset $D_{3h\tilde{\sigma}\tilde{I}}$ are obtained by the GAP code `elm_D3h*(1,4)(2,5)(3,6)`, where the symbol `elm_D3h` represents the GAP list for the set of elements of D_{3h} (cf. the D_{3h} -part of Table 1). The set of the elements of $D_{3h\tilde{\sigma}\tilde{I}}$ is obtained in the form of a GAP list named `elm_D3hsI`, where the GAP function

Concatenation is used. The resulting list `e1m_D3hsI` is consistent with the data collected in the $D_{3h\tilde{\sigma}\tilde{\tau}}$ -part of Figure 1. The list `e1m_D3hsI` can be transformed into a group `D3hsI` by using the GAP function `AsGroup`. Thereby, the combined representation `D3hsI` is regarded as a permutation group.

3.2.2 Combined representation `cD3hsI` for the stereoisomeric group $\tilde{D}_{3h\tilde{\sigma}\tilde{\tau}}$

The construction of the stereoisomeric group $\tilde{D}_{3h\tilde{\sigma}\tilde{\tau}}$ on the basis of the combined representations is shown in the $\tilde{D}_{3h\tilde{\sigma}\tilde{\tau}}$ -part of Table 2, which collects the GAP codes for generating the combined representation `cD3hsI` according to Eq. 8. Thus, the elements of the coset $D_{3h\tilde{\sigma}\tilde{\tau}}\tilde{\sigma}_{14}$ are calculated by the GAP code `e1m_D3hsI*(1,4)`, those of the coset $D_{3h\tilde{\sigma}\tilde{\tau}}\tilde{\sigma}_{25}$ are calculated by the GAP code `e1m_D3hsI*(2,5)`, and those of the coset $D_{3h\tilde{\sigma}\tilde{\tau}}\tilde{\sigma}_{36}$ are calculated by the GAP code `e1m_D3hsI*(3,5)`, where the symbol `e1m_D3hsI` represents the GAP list for the set of elements of $D_{3h\tilde{\sigma}\tilde{\tau}}$ (cf. the $D_{3h\tilde{\sigma}\tilde{\tau}}$ -part of Table 1). The set of the elements of $\tilde{D}_{3h\tilde{\sigma}\tilde{\tau}}$ is obtained in the form of a GAP list named `e1m_cD3hsI`, where the GAP function `Concatenation` is used. The resulting list `e1m_cD3hsI` is consistent with the whole data collected in Figure 1. The list `e1m_cD3hsI` can be transformed into a group `cD3hsI` by using the GAP function `AsGroup`. Thereby, the combined representation `cD3hsI` is regarded as a permutation group.

3.2.3 Combined representation `ccD3hsI` for the isoskeletal group $\tilde{\tilde{D}}_{3h\tilde{\sigma}\tilde{\tau}}$

The isoskeletal group $\tilde{\tilde{D}}_{3h\tilde{\sigma}\tilde{\tau}}$ is constructed according to Eq. 10. The corresponding combined representation `ccD3hsI` is shown in the $\tilde{\tilde{D}}_{3h\tilde{\sigma}\tilde{\tau}}$ -part of Table 2. The transversals listed in Eq. 9 are used in the GAP function `Concatenation`, so as to give a GAP list named `e1m_ccD3hsI`. The list `e1m_ccD3hsI` can be transformed into a group `ccD3hsI` by using the GAP function `AsGroup`. Thereby, the combined representation `ccD3hsI` is regarded as a permutation group.

The isoskeletal group $\tilde{\tilde{D}}_{3h\tilde{\sigma}\tilde{\tau}}$ (the combined representation as a group: `ccD3hsI`) is isomorphic to the reflective symmetric group $S_{\sigma\tilde{\tau}}^{[6]}$ (the combined representation as a group: `S6sI`), which is generated by adding a reflection (7,8) to the symmetric group of degree 6 ($S^{[6]}$, the combined representation as a group `S6`). The isomorphism between `ccD3hsI` and `S6sI` is confirmed by the following GAP code:

```
gap> #Isoskeletal Group;;
gap> ccD3hsI := Group([ (7,8), (5,6), (4,5), (3,4), (2,3), (1,2) ]);
Group([ (7,8), (5,6), (4,5), (3,4), (2,3), (1,2) ])
gap> Size(ccD3hsI);
```

Table 2. Group Hierarchy for Characterizing a Cyclopropane Skeleton (Part 2)

group	list of elements for constructing a group
$\widetilde{D}_{3h\bar{\sigma}I}$ (stereo- isomeric group) order: 96	<pre> gap> #Stereoisomeric group;; gap> elm_cD3hsI := Concatenation(elm_D3hsI, elm_D3hsI*(1,4), elm_D3hsI*(2,5), elm_D3hsI*(3,6)); [(omitted: elm_D3hsI) (1,4), (1,2,3,4,5,6), (1,3,2,4,6,5), (2,6)(3,5), (1,6,4,3)(2,5), (1,5,4,2)(3,6), (2,5)(3,6)(7,8), (1,5,3)(2,6,4)(7,8), (1,6,2)(3,5,4)(7,8), (1,4)(2,3)(5,6)(7,8), (1,3,4,6)(7,8), (1,2,4,5)(7,8), (2,5)(3,6), (1,5,3)(2,6,4), (1,6,2)(3,5,4), (1,4)(2,3)(5,6), (1,3,4,6), (1,2,4,5), (1,4)(7,8), (1,2,3,4,5,6)(7,8), (1,3,2,4,6,5)(7,8), (2,6)(3,5)(7,8), (1,6,4,3)(2,5)(7,8), (1,5,4,2)(3,6)(7,8), (2,5), (1,5,6,4,2,3), (1,3,5,4,6,2), (1,4)(2,6,5,3), (1,6)(3,4), (1,2,4,5)(3,6), (1,4)(3,6)(7,8), (1,2,6)(3,4,5)(7,8), (1,6,5)(2,4,3)(7,8), (2,3,5,6)(7,8), (1,3)(2,5)(4,6)(7,8), (1,5,4,2)(7,8), (1,4)(3,6), (1,2,6)(3,4,5), (1,6,5)(2,4,3), (2,3,5,6), (1,3)(2,5)(4,6), (1,5,4,2), (2,5)(7,8), (1,5,6,4,2,3)(7,8), (1,3,5,4,6,2)(7,8), (1,4)(2,6,5,3)(7,8), (1,6)(3,4)(7,8), (1,2,4,5)(3,6)(7,8), (3,6), (1,2,6,4,5,3), (1,6,5,4,3,2), (1,4)(2,3,5,6), (1,3,4,6)(2,5), (1,5)(2,4), (1,4)(2,5)(7,8), (1,5,6)(2,3,4)(7,8), (1,3,5)(2,4,6)(7,8), (2,6,5,3)(7,8), (1,6,4,3)(7,8), (1,2)(3,6)(4,5)(7,8), (1,4)(2,5), (1,5,6)(2,3,4), (1,3,5)(2,4,6), (2,6,5,3), (1,6,4,3), (1,2)(3,6)(4,5), (3,6)(7,8), (1,2,6,4,5,3)(7,8), (1,6,5,4,3,2)(7,8), (1,4)(2,3,5,6)(7,8), (1,3,4,6)(2,5)(7,8), (1,5)(2,4)(7,8)] gap> cD3hsI := AsGroup(elm_cD3hsI); Group([(7,8), (3,6), (2,3)(5,6), (1,2)(4,5)]) gap> Print("IsEqualSet(elm_cD3hsI, Elements(cD3hsI))_?:_", IsEqualSet(↪ elm_cD3hsI, Elements(cD3hsI)), "\n"); IsEqualSet(elm_cD3hsI, Elements(cD3hsI)) ? : true gap> Print("Order_of_ℓcD3hsI:_", Size(cD3hsI), "\n"); Order of cD3hsI: 96 </pre>
$\widetilde{D}_{3h\bar{\sigma}I}$ (isoskeletal group) order: 1440	<pre> gap> #Isoskeletal group;; gap> elm_ccD3hsI := Concatenation(elm_cD3hsI, elm_cD3hsI*(5,6), > elm_cD3hsI*(4,5), elm_cD3hsI*(4,5,6), elm_cD3hsI*(4,6,5), > elm_cD3hsI*(4,6), elm_cD3hsI*(3,4), elm_cD3hsI*(3,4)(5,6), > elm_cD3hsI*(3,4,5), elm_cD3hsI*(3,4,6,5), elm_cD3hsI*(3,5,4), > elm_cD3hsI*(3,5), elm_cD3hsI*(2,3,4), elm_cD3hsI*(2,3,4)(5,6), ↪ elm_cD3hsI*(2,3,5,4)); [(), (1,2,3)(4,5,6), (1,3,2)(4,6,5), (1,4)(2,6)(3,5), (1,6)(2,5)(3,4), (1,5)(2,4)(3,6), (1,4)(2,5)(3,6)(7,8), (omitted) (1,5,3,2,4,6), (1,4,3,5), (1,2,4)(3,5)(7,8), (1,4,3,2,5,6)(7,8), ↪ (1,5)(3,4,6)(7,8), (2,6,4)(7,8), (1,6,2,3)(4,5)(7,8), (1,3,6,5,2)(7,8), (1,2,4)(3,5), (1,4,3,2,5,6), ↪ (1,5)(3,4,6), (2,6,4), (1,6,2,3)(4,5), (1,3,6,5,2), (2,3,6,5,4)(7,8), (1,3)(2,6)(7,8), (1,6,4,5,2)(7,8), ↪ (1,2,5,6,3,4)(7,8), (1,5,3,2,4,6)(7,8), (1,4,3,5)(7,8)] gap> ccD3hsI := AsGroup(elm_ccD3hsI); Group([(7,8), (5,6), (4,5), (3,4), (2,3), (1,2)]) gap> Print("IsEqualSet(elm_ccD3hsI, Elements(ccD3hsI))_?:_", ↪ IsEqualSet(elm_ccD3hsI, Elements(ccD3hsI)), "\n"); IsEqualSet(elm_ccD3hsI, Elements(ccD3hsI)) ? : true gap> Print("Order_of_ℓccD3hsI:_", Size(ccD3hsI), "\n"); Order of ccD3hsI: 1440 </pre>

```

1440
gap> #Symmetric Group of Degree 6;;
gap> S6 := Group([(1,2,3,4,5,6), (1,2)]);
Group([ (1,2,3,4,5,6), (1,2) ])
gap> Size(S6);
720
gap> #Reflective symmetric group S6sI;;
gap> S6sI := Group([(1,2,3,4,5,6), (1,2), (7,8)]);
Group([ (1,2,3,4,5,6), (1,2), (7,8) ])
gap> Size(S6sI);
1440
gap> IsEqualSet(Elements(ccD3hsI), Elements(S6sI));
true

```

Note that the isoskeletal group `ccD3hsI` is generated by the GAP function `Group` in accord with the generators shown in the $\widetilde{D}_{3h\bar{\sigma}\bar{I}}$ -part of Table 2. The final output `true` shows that the set of elements calculated by `Elements(ccD3hsI)` is identical with the set of elements calculated by `Elements(S6sI)`.

4 Hierarchical enumeration of cyclopropane derivatives

Hierarchical enumeration of cyclopropane derivatives is conducted by extending Fujita's proligand method [11–14], which has been originally developed for point groups. The procedures of calculating cycle indices with chirality fittingness (CI-CFs) for point groups can be easily extended to cover the hierarchical enumeration.

4.1 Calculation of CI-CFs

Fujita's proligand method [11–14] is based on a cycle index with chirality fittingness (CI-CF). Such a CI-CF is manually calculated from the products of sphericity indices (PSIs) for the respective elements, where the PSIs are in turn calculated by the examination of the cycle structures of the respective elements. For example, the D_{3h} -part (the D_{3p} -part plus $D_{3\sigma h}$ -part) of Figure 1 indicates the cycle structures of respective elements and the corresponding PSIs, where a sphericity index (SI) b_d is assigned to a hemispheric d -cycle, an SI a_d to a homospheric d -cycle (d : odd), and an SI c_d to an enantiospheric d -cycle (d : even). These PSIs are summed up and divided by the order of the point group D_{3h} (order: $|D_{3h}| = 12$), so as to give the following CI-CF:

$$\text{CI-CF}(D_{3h}, \$_d) = \frac{1}{12} (b_1^6 + 2b_3^2 + 3b_2^3 + c_2^3 + 2c_6 + 3a_1^2 c_2^2), \quad (13)$$

where the symbol $\$_d$ indicates b_d , a_d , or c_d .

The manual calculation of the CI-CF described in the preceding paragraph can be systematically conducted by using the combined-permutation representation [24], where the GAP function `CalcConjClassCICF` has been developed for the purpose of calculating CI-CFs [25]. The CI-CF shown in Eq. 13 is alternatively by using `CalcConjClassCICF` as follows:

```
gap> Read("c:/fujita0/fujita2017/D3hsI-GAP/cal-c-GAP/CICFgenCC.gapfunc");
gap> D3h := Group([(2,3)(5,6)(7,8), (1,2)(4,5)(7,8), (1,4)(2,5)(3,6)(7,8)]);;
gap> Print("D3h:=_", D3h, "\n");
D3h := Group( [ (2,3)(5,6)(7,8), (1,2)(4,5)(7,8), (1,4)(2,5)(3,6)(7,8) ] )
gap> Print("Order:=_", Size(D3h), "\n");
Order := 12
gap> Print("CICF_D3h:=_", CalcConjClassCICF(D3h, 6, 8), "\n");
CICF_D3h := 1/12*b_1^6+1/4*a_1^2*c_2^2+1/12*c_2^3+1/4*b_2^3+1/6*b_3^2+1/6*c_c
```

Each GAP code after the prompt `gap>` is executed to give the output in the next line, which is taken up to print each line in the D_{3h} -part of Table 3. In the GAP calculation described above, the set of generators shown in the D_{3h} -part of Table 2 is used to generate the combined representation `D3h` as a group. Note that the GAP function `CalcConjClassCICF` is stored in the file `CICFgenCC.gapfunc`, which is placed in an appropriate directory named `c:/fujita0/fujita2017/D3hsI-GAP/cal-c-GAP/`. The file `CICFgenCC.gapfunc` is loaded by the GAP function `Read`. The calculated CI-CF (`CICF_D3h`) is consistent with Eq. 13, which has been obtained manually.

Similarly, the CI-CFs for the groups listed hierarchically in Tables 1 and 2 are obtained by using the GAP function `CalcConjClassCICF`. The calculated CI-CFs are collected hierarchically in Table 3. These CI-CFs (except the isoskeletal group) can be calculated manually by using the data of PSIs collected in Figure 1.

4.2 Enumerations under the point groups D_3 and D_{3h} as well as under the RS -stereoisomeric group $D_{3h\bar{\sigma}\hat{I}}$

4.2.1 Ligand-inventory functions for 3D enumeration

Let us select proligands for enumerating cyclopropane derivatives from the following ligand inventory for 3D enumeration:

$$\mathbf{L}_{3D} = \{H, A, B, C, D, V; p, \bar{p}, q, \bar{q}, r, \bar{r}, s, \bar{s}, t, \bar{t}, u, \bar{u}\}, \quad (14)$$

where the uppercase letters H, A, B, C, D, and V represent achiral proligands, while a pair of lowercase letters p/\bar{p} , q/\bar{q} , r/\bar{r} , s/\bar{s} , t/\bar{t} , or u/\bar{u} represents an enantiomeric pair of chiral proligands in isolation (when detached).

Table 3. CI-CFs for Characterizing a Cyclopropane Skeleton

group	Group due to a list of generators, order, CI-CF
D_3 (point group)	D3 := Group([(1,2,3)(4,5,6), (1,4)(2,6)(3,5)]) Order := 6 CICF_D3 := 1/6*b ₁ ⁶ +1/2*b ₂ ³ +1/3*b ₃ ²
D_{3h} (point group)	D3h := Group([(2,3)(5,6)(7,8), (1,2)(4,5)(7,8), (1,4)(2,5)(3,6)(7,8)]) Order := 12 CICF_D3h := 1/12*b ₁ ⁶ +1/4*a ₁ ² *c ₂ ² +1/4*b ₂ ³ +1/12*c ₂ ³ +1/6*b ₃ ² +1/6*c ₆
$D_{3h\bar{\sigma}\bar{\tau}}$ (<i>RS</i> -stereo- isomeric group)	D3hsI := Group([(7,8), (2,3)(5,6), (1,2)(4,5), (1,4)(2,5)(3,6)]) Order := 24 CICF_D3hsI := 1/24*b ₁ ⁶ +1/24*a ₁ ⁶ +1/8*b ₁ ² *b ₂ ² +1/8*a ₁ ² *c ₂ ² +1/6*b ₂ ³ +1/6*c ₂ ³ +1/12*b ₃ ² +1/12*a ₃ ² +1/12*c ₆ +1/12*b ₆
$\tilde{D}_{3h\bar{\sigma}\bar{\tau}}$ (stereoisomeric group)	cd3hsI := Group([(7,8), (3,6), (2,3)(5,6), (1,2)(4,5)]) Order := 96 CICF_cd3hsI := 1/96*b ₁ ⁶ +1/96*a ₁ ⁶ +1/32*b ₁ ⁴ *b ₂ +1/32*a ₁ ⁴ *c ₂ +3/32*b ₁ ² *b ₂ ² +3/32*a ₁ ² *c ₂ ² +1/16*b ₁ ² *b ₄ +7/96*b ₂ ³ +1/16*a ₁ ² *c ₄ +7/96*c ₂ ³ +1/12*b ₃ ² +1/16*b ₂ *b ₄ +1/16*c ₂ *c ₄ +1/12*a ₃ ² +1/12*c ₆ +1/12*b ₆
$\tilde{\tilde{D}}_{3h\bar{\sigma}\bar{\tau}}$ (isoskeletal group)	ccd3hsI := Group([(7,8), (5,6), (4,5), (3,4), (2,3), (1,2)]) Order := 1440 CICF_ccd3hsI := 1/1440*b ₁ ⁶ +1/1440*a ₁ ⁶ +1/96*b ₁ ⁴ *b ₂ +1/96*a ₁ ⁴ *c ₂ +1/36*b ₁ ³ *b ₃ +1/32*b ₁ ² *b ₂ ² +1/36*a ₁ ³ *a ₃ +1/32*a ₁ ² *c ₂ ² +1/16*b ₁ ² *b ₄ +1/12*b ₁ *b ₃ *b ₂ +1/96*b ₂ ³ +1/16*a ₁ ² *c ₄ +1/12*a ₁ *c ₂ *a ₃ +1/96*c ₂ ³ +1/10*b ₁ *b ₅ +1/36*b ₃ ² +1/16*b ₂ *b ₄ +1/10*a ₁ *a ₅ +1/16*c ₂ *c ₄ +1/36*a ₃ ² +1/12*c ₆ +1/12*b ₆

Suppose that the six positions of a cyclopropane skeleton **1** (cf. Eq. 11) accommodate a set of six proligands selected from the ligand inventory \mathbf{L}_{3D} (Eq. 14). According to Fujita's proligand method [11–14], the following set of ligand-inventory functions are adopted:

$$a_d = H^d + A^d + B^d + C^d + D^d + V^d \quad (15)$$

$$c_d = H^d + A^d + B^d + C^d + D^d + V^d \\ + 2p^{d/2}\bar{p}^{d/2} + 2q^{d/2}\bar{q}^{d/2} + 2r^{d/2}\bar{r}^{d/2} + 2s^{d/2}\bar{s}^{d/2} + 2t^{d/2}\bar{t}^{d/2} + 2u^{d/2}\bar{u}^{d/2} \quad (16)$$

$$b_d = H^d + A^d + B^d + C^d + D^d + V^d \\ + p^d + \bar{p}^d + q^d + \bar{q}^d + r^d + \bar{r}^d + s^d + \bar{s}^d + t^d + \bar{t}^d + u^d + \bar{u}^d, \quad (17)$$

where the symbol d represents a non-negative integer.

The introduction of the ligand-inventory functions (Eqs. 15–17) into the CI-CF(D_3 , b_d) (CICF_D3 shown in Table 3) or the CI-CF(D_{3h} , $\$d$) (CICF_D3h shown in Table 3) enables us to conduct enumeration under the point group D_3 or under the point group D_{3h} . Because the enumeration under the point group D_{3h} differentiates the two chiral proligands of a

single enantiomeric pair (e.g., p vs. \bar{p}), the ligand-inventory function for c_d (Eq. 16) takes account of two modes of packing in the case of an enantiospheric cycle. As a result, a promolecule containing $p\bar{p}$, for example, is counted separately apart from a promolecule containing p^2 (or \bar{p}^2).

For the purpose of hierarchical enumeration, such pairwise chiral proligands (i.e., p vs. \bar{p} etc.) are bundled into a single symbol, i.e., \check{p} etc., whereas such two modes of packing are maintained in accord with the ligand inventory \mathbf{L}_{3D} (Eq. 14). It follows that the ligand-inventory functions (Eqs. 15–17) are transformed by putting $\check{p} = p = \bar{p}$ into the following ligand-inventory functions for 3D enumeration:

$$a_d = H^d + A^d + B^d + C^d + D^d + V^d \quad (18)$$

$$c_d = H^d + A^d + B^d + C^d + D^d + V^d + 2\check{p}^d + 2\check{q}^d + 2\check{r}^d + 2\check{s}^d + 2\check{t}^d + 2\check{u}^d \quad (19)$$

$$b_d = H^d + A^d + B^d + C^d + D^d + V^d + 2\check{p}^d + 2\check{q}^d + 2\check{r}^d + 2\check{s}^d + 2\check{t}^d + 2\check{u}^d. \quad (20)$$

4.2.2 Generating functions for point groups and *RS*-stereoisomeric groups

For the purpose of enumerating cyclopropane derivatives under the point group \mathbf{D}_3 , the ligand-inventory function (Eq. 20) is introduced into the CI-CF(\mathbf{D}_3, b_d) (CICF_D3) shown in Table 3). Thereby, we are able to obtain the following generating function:

$$\sum_{\theta} T_{(\mathbf{D}_3)\check{\theta}} W_{\check{\theta}} = \text{CI-CF}(\mathbf{D}_3, b_d) \Big|_{\text{Eq. 20}}, \quad (21)$$

where the coefficient $T_{(\mathbf{D}_3)\check{\theta}}$ of the weight $W_{\check{\theta}}$ indicates the number of cyclopropane derivatives with the composition $W_{\check{\theta}}$. Each 3D entity is inequivalent with another 3D entity under the point group \mathbf{D}_3 so that it is counted once separately. The weight $W_{\check{\theta}}$ is represented by the symbol $H^h A^a B^b C^c D^d V^v \check{p}^{\check{p}} \check{q}^{\check{q}} \check{r}^{\check{r}} \check{s}^{\check{s}} \check{t}^{\check{t}} \check{u}^{\check{u}}$, where the powers satisfy the following equation:

$$h + a + b + c + d + v + \check{p} + \check{q} + \check{r} + \check{s} + \check{t} + \check{u} = 6. \quad (22)$$

For the sake of convenience, the weight $W_{\check{\theta}}$ is represented by the partition $[\check{\theta}]$ as follows:

$$[\check{\theta}] = [h, a, b, c, d, v, \check{p}, \check{q}, \check{r}, \check{s}, \check{t}, \check{u}], \quad (23)$$

which satisfies $h \geq a \geq b \geq c \geq d \geq v$; and $\check{p} \geq \check{q} \geq \check{r} \geq \check{s} \geq \check{u} \geq \check{t}$, because respective terms appear symmetrically in such generating functions as Eq. 21.

On the other hand, the enumeration of cyclopropane derivatives under the point group \mathbf{D}_{3h} is conducted by the introduction of the ligand-inventory functions (Eqs. 18–20) into

the CI-CF(\mathbf{D}_{3h} , \mathbb{S}_d) (CICF_D3h) shown in Table 3. Thereby, the following generating function is obtained:

$$\sum_{\theta} B_{(\mathbf{D}_{3h})\tilde{\theta}} W_{\tilde{\theta}} = \text{CI-CF}(\mathbf{D}_{3h}, \mathbb{S}_d) \Big|_{\text{Eqs. 18-20}}, \quad (24)$$

where the coefficient $B_{(\mathbf{D}_{3h})\tilde{\theta}}$ of the weight $W_{\tilde{\theta}}$ indicates the number of pairs of enantiomeric cyclopropane derivatives with the composition $W_{\tilde{\theta}}$. The inequivalence under the point group \mathbf{D}_{3h} means that each pair of (self-)enantiomeric cyclopropane derivatives is counted once under this enumeration. Note that a pair of self-enantiomers means an achiral cyclopropane derivative.

The procedure for the enumeration under the point groups \mathbf{D}_3 and \mathbf{D}_{3h} can be extended to cover the enumeration under the *RS*-stereoisomeric group $\mathbf{D}_{3h\tilde{\sigma}\hat{\Gamma}}$. Accordingly, the same set of ligand-inventory functions (Eqs. 18–20) is introduced into CI-CF($\mathbf{D}_{3h\tilde{\sigma}\hat{\Gamma}}$, \mathbb{S}_d) (CICF_D3hsI) shown in Table 3. Thereby, the following generating function is obtained:

$$\sum_{\theta} B_{(\mathbf{D}_{3h\tilde{\sigma}\hat{\Gamma}})\tilde{\theta}} W_{\tilde{\theta}} = \text{CI-CF}(\mathbf{D}_{3h\tilde{\sigma}\hat{\Gamma}}, \mathbb{S}_d) \Big|_{\text{Eqs. 18-20}}, \quad (25)$$

where the coefficient $B_{(\mathbf{D}_{3h\tilde{\sigma}\hat{\Gamma}})\tilde{\theta}}$ of the weight $W_{\tilde{\theta}}$ indicates the number of quadruplets of *RS*-stereoisomeric cyclopropane derivatives with the composition $W_{\tilde{\theta}}$. Each quadruplet of *RS*-stereoisomeric cyclopropane derivatives is counted once under this enumeration in accord with the inequivalence under the *RS*-stereoisomeric group $\mathbf{D}_{3h\tilde{\sigma}\hat{\Gamma}}$.

4.3 Enumerations under the stereoisomeric group $\tilde{\mathbf{D}}_{3h\tilde{\sigma}\hat{\Gamma}}$ and under the isoskeletal group $\tilde{\tilde{\mathbf{D}}}_{3h\tilde{\sigma}\hat{\Gamma}}$

4.3.1 A single ligand–inventory function for graph enumeration

In the discussion on stereoisomers and isoskeletomers, each pair of enantiomeric proligands in isolation degenerates into a single graph, because they are 2D-based concepts. Thus, a pair of p/\bar{p} , q/\bar{q} , r/\bar{r} , s/\bar{s} , t/\bar{t} , or u/\bar{u} is considered to coincide into \check{p} , \check{q} , \check{r} , \check{s} , \check{t} , or \check{u} , each of which is regarded as a single graph without obeying the above mentioned sphericities. As a result, the ligand inventory \mathbf{L}_{3D} (Eq. 14) is transformed into the following ligand inventory for graph enumeration:

$$\mathbf{L}_{2D} = \{H, A, B, C, D, V; \check{p}, \check{q}, \check{r}, \check{s}, \check{t}, \check{u}\}, \quad (26)$$

where the uppercase letters H, A, B, C, D, and V represent achiral proligands, while the symbols \check{p} , \check{q} , \check{r} , \check{s} , \check{t} , and \check{u} represent graphs generated from p/\bar{p} , q/\bar{q} , r/\bar{r} , and s/\bar{s} , t/\bar{t} , and u/\bar{u} .

A set of six proligands selected from the ligand inventory \mathbf{L}_{2D} (Eq. 26) is placed on the six positions of the cyclopropane skeleton $\mathbf{1}$, which is now regarded as degenerating into a graph. This means that the six positions are considered to be controlled by the stereoisomeric group $\tilde{\mathbf{D}}_{3h\bar{\sigma}\hat{\Gamma}}$ or the isoskeletal group $\tilde{\tilde{\mathbf{D}}}_{3h\bar{\sigma}\hat{\Gamma}}$. Because the elements of \mathbf{L}_{2D} (Eq. 26) are graphs even if they are derived from either achiral or chiral proligands, a single ligand-inventory function for graph enumeration is obtained as follows:

$$a_d = c_d = b_d = H^d + A^d + B^d + C^d + D^d + V^d + \check{p}^d + \check{q}^d + \check{r}^d + \check{s}^d + \check{i}^d + \check{u}^d. \quad (27)$$

Note that the term $2\check{p}^d$ etc. in Eqs. 19 and 20 for 3D enumeration are replaced by the term \check{p}^d etc. in Eq. 27 for graph enumeration.

4.3.2 Calculation of generating functions for stereoisomeric groups and isoskeletal groups

The ligand-inventory function (Eq. 27) is introduced into CI-CF($\tilde{\mathbf{D}}_{3h\bar{\sigma}\hat{\Gamma}}, \mathbb{S}_d$) (CICF_cD3hsI) shown in Table 3. Thereby, the following generating function is obtained:

$$\sum_{\check{\theta}} B_{(\tilde{\mathbf{D}}_{3h\bar{\sigma}\hat{\Gamma}})\check{\theta}} W_{\check{\theta}} = \text{CI-CF}(\tilde{\mathbf{D}}_{3h\bar{\sigma}\hat{\Gamma}}, \mathbb{S}_d) \Big|_{\text{Eq. 27}}. \quad (28)$$

The coefficient $B_{(\tilde{\mathbf{D}}_{3h\bar{\sigma}\hat{\Gamma}})\check{\theta}}$ of the weight $W_{\check{\theta}}$ in the generating function (Eq. 28) indicates the number of sets of stereoisomeric cyclopropane derivatives with the composition $W_{\check{\theta}}$. Thus, each set of stereoisomeric cyclopropane derivatives is counted once under the stereoisomeric group $\tilde{\mathbf{D}}_{3h\bar{\sigma}\hat{\Gamma}}$.

On the other hand, the ligand-inventory function (Eq. 27) is introduced into the CI-CF($\tilde{\tilde{\mathbf{D}}}_{3h\bar{\sigma}\hat{\Gamma}}, \mathbb{S}_d$) (CICF_ccD3hsI listed in Table 3), so as to give the following generating function:

$$\sum_{\check{\theta}} B_{(\tilde{\tilde{\mathbf{D}}}_{3h\bar{\sigma}\hat{\Gamma}})\check{\theta}} W_{\check{\theta}} = \text{CI-CF}(\tilde{\tilde{\mathbf{D}}}_{3h\bar{\sigma}\hat{\Gamma}}, \mathbb{S}_d) \Big|_{\text{Eq. 27}}, \quad (29)$$

where the coefficient $B_{(\tilde{\tilde{\mathbf{D}}}_{3h\bar{\sigma}\hat{\Gamma}})\check{\theta}}$ of the weight $W_{\check{\theta}}$ indicates the number of sets of isoskeletal cyclopropane derivatives with the composition $W_{\check{\theta}}$. Because the enumerated sets of isoskeletomers are inequivalent with each other under the isoskeletal group $\tilde{\tilde{\mathbf{D}}}_{3h\bar{\sigma}\hat{\Gamma}}$, each of the sets is counted once under this enumeration.

4.4 Results of enumeration

4.4.1 GAP-calculation of generating functions

The generating functions shown in Eqs. 21, 24, 25, 28, and 29 are practically calculated by writing the GAP codes. The coefficients are extracted from the generating functions and listed in tabular forms (Appendix A). Among the data shown in tabular forms, the $T_{(\mathbf{D}_3)\bar{\theta}}$ -column (due to Eq. 21), the $B_{(\mathbf{D}_{3h})\bar{\theta}}$ -column (due to Eq. 24), and the $B_{(\mathbf{D}_{3h\bar{\sigma}})\bar{\theta}}$ -column (due to 25) are concerned with 3D structures, where the set of ligand-inventory functions (Eqs. 18–20) is used. On the other hand the $B_{(\tilde{\mathbf{D}}_{3h\bar{\sigma}})\bar{\theta}}$ -column (due to Eq. 28) and the $B_{(\tilde{\tilde{\mathbf{D}}}_{3h\bar{\sigma}})\bar{\theta}}$ -column (due to Eq. 29) are concerned with graphs, where the single ligand-inventory function (Eq. 27) is used.

4.4.2 Cyclopropane derivatives with achiral proligands

Table 4 shows selected data, which are obtained by adopting achiral proligands and no chiral proligands, where the partitions $[\dot{\theta}]_1 - [\ddot{\theta}]_{11}$ are used. Note that the six integers at the first part of each partition are concerned with achiral proligands, while the six integers at the next part are concerned with chiral proligands (cf. Eq. 23).

Table 4. Hierarchical Enumeration of Cyclopropane Derivatives with Achiral Proligands and No Chiral Proligands

partition	numbers of cyclopropane derivatives under respective groups				
	$T_{(\mathbf{D}_3)\bar{\theta}}$ (Eq. 21)	$B_{(\mathbf{D}_{3h})\bar{\theta}}$ (Eq. 24)	$B_{(\mathbf{D}_{3h\bar{\sigma}})\bar{\theta}}$ (Eq. 25)	$B_{(\tilde{\mathbf{D}}_{3h\bar{\sigma}})\bar{\theta}}$ (Eq. 28)	$B_{(\tilde{\tilde{\mathbf{D}}}_{3h\bar{\sigma}})\bar{\theta}}$ (Eq. 29)
	Eqs. 18–20			Eq. 27	
$[\dot{\theta}]_1 = [6, 0, 0, 0, 0, 0, 0, 0, 0, 0, 0]$	1	1	1	1	1
$[\dot{\theta}]_2 = [5, 1, 0, 0, 0, 0, 0, 0, 0, 0, 0]$	1	1	1	1	1
$[\dot{\theta}]_3 = [4, 2, 0, 0, 0, 0, 0, 0, 0, 0, 0]$	4	3	3	2	1
$[\dot{\theta}]_4 = [4, 1, 1, 0, 0, 0, 0, 0, 0, 0, 0]$	5	3	3	2	1
$[\dot{\theta}]_5 = [3, 3, 0, 0, 0, 0, 0, 0, 0, 0, 0]$	4	3	3	2	1
$[\dot{\theta}]_6 = [3, 2, 1, 0, 0, 0, 0, 0, 0, 0, 0]$	10	6	6	3	1
$[\dot{\theta}]_7 = [3, 1, 1, 1, 0, 0, 0, 0, 0, 0, 0]$	20	10	10	4	1
$[\dot{\theta}]_8 = [2, 2, 2, 0, 0, 0, 0, 0, 0, 0, 0]$	18	11	11	5	1
$[\dot{\theta}]_9 = [2, 2, 1, 1, 0, 0, 0, 0, 0, 0, 0]$	30	16	16	6	1
$[\dot{\theta}]_{10} = [2, 1, 1, 1, 1, 0, 0, 0, 0, 0, 0]$	60	30	30	9	1
$[\dot{\theta}]_{11} = [1, 1, 1, 1, 1, 1, 0, 0, 0, 0, 0]$	120	60	60	15	1

To confirm the validity of Table 4, let us examine the data shown in the $[\tilde{\theta}]_3$ -row, which collects the results for the composition H^4A^2 . Suppose that four hydrogens and two achiral proligands A's are placed on the six positions of the reference skeleton **1** shown in Figure 1 in accord with the following function:

$$f_1 : f_1(1) = f_1(5) = A; f_1(2) = f_1(3) = f_1(4) = f_1(6) = H, \quad (30)$$

where each integer in a pair of parentheses indicates the locant number of the skeleton **1**. Thereby, Figure 2 is obtained under the action of the point groups D_3 and D_{3h} ; the RS -stereoisomeric group $D_{3h\tilde{\sigma}\tilde{\tau}}$; as well as under the stereoisomeric group $\tilde{D}_{3h\tilde{\sigma}\tilde{\tau}}$. Thus, the $D_{3h\tilde{\sigma}\tilde{\tau}}$ -part of Figure 1 generates the corresponding type-I stereoisogram, which consists of a quadruplet of RS -stereoisomers, i.e., a reference **9**, an RS -diastereomer **10** ($= \bar{\mathbf{9}}$), an enantiomer $\bar{\mathbf{9}}$, and a holantimer $\overline{\mathbf{10}}$ ($= \mathbf{9}$). Note that this quadruplet of RS -stereoisomers degenerates into a pair of enantiomers $\mathbf{9}/\bar{\mathbf{9}}$, which represents a pair of enantiomeric *trans*-cyclopropanes.

On the other hand, the $D_{3h\tilde{\sigma}\tilde{\tau}}\hat{\sigma}_{14}$ -part of Figure 1 generates the corresponding type-IV stereoisogram. This stereoisogram consists of a quadruplet of RS -stereoisomers which degenerates into a single achiral cyclopropane **11**.

The $D_{3h\tilde{\sigma}\tilde{\tau}}\hat{\sigma}_{25}$ -part (or the $D_{3h\tilde{\sigma}\tilde{\tau}}\hat{\sigma}_{36}$ -part) of Figure 1 generates a stereoisogram which degenerates into the above-mentioned type-IV stereoisogram (or type-I stereoisogram). This feature is represented schematically $I^2 - IV^2$, where the power 2 of I means that two type-I stereoisograms degenerate into a single stereoisogram and the power 2 of IV means that two type-IV stereoisograms degenerate into a single stereoisogram.

In summary, under the action of the stereoisomeric group $\tilde{D}_{3h\tilde{\sigma}\tilde{\tau}}$ (Figure 1), there remain the two stereoisograms, which show stereoisomerism (*cis/trans*-isomerism) between the pair of enantiomeric *trans*-cyclopropanes $\mathbf{9}/\bar{\mathbf{9}}$ and the achiral *cis*-cyclopropane **11**.

Figure 2 also shows the action of the isoskeletal group $\tilde{\tilde{D}}_{3h\tilde{\sigma}\tilde{\tau}}$ (Figure 1), which shows the coset decomposition of Eq. 10. Among the transversals listed in Eq. 9, eleven transversals, i.e., $\tilde{\sigma}_{56}$, $\tilde{\sigma}_{465}$, $\tilde{\sigma}_{46}$, $\tilde{\sigma}_{34}$, $\tilde{\sigma}_{34,56}$, $\tilde{\sigma}_{3465}$, $\tilde{\sigma}_{354}$, $\tilde{\sigma}_{35}$, $\tilde{\sigma}_{234}$, $\tilde{\sigma}_{234,56}$, and $\tilde{\sigma}_{2354}$ (in addition to the transversal I of the coset $\tilde{\tilde{D}}_{3h\tilde{\sigma}\tilde{\tau}}I$) exhibits degeneration, which is summarized by the scheme $(I^2 - IV^2)^{12}$.

On the other hand, the $\tilde{\tilde{D}}_{3h\tilde{\sigma}\tilde{\tau}}\tilde{\sigma}_{45}$ -part of Figure 2 shows that the action of the isoskeletal group $\tilde{\tilde{D}}_{3h\tilde{\sigma}\tilde{\tau}}$ generates a type-IV stereoisogram, which shows a single achiral cyclopropane **13**. This mode of degeneration is indicated by the scheme IV^4 . Among the

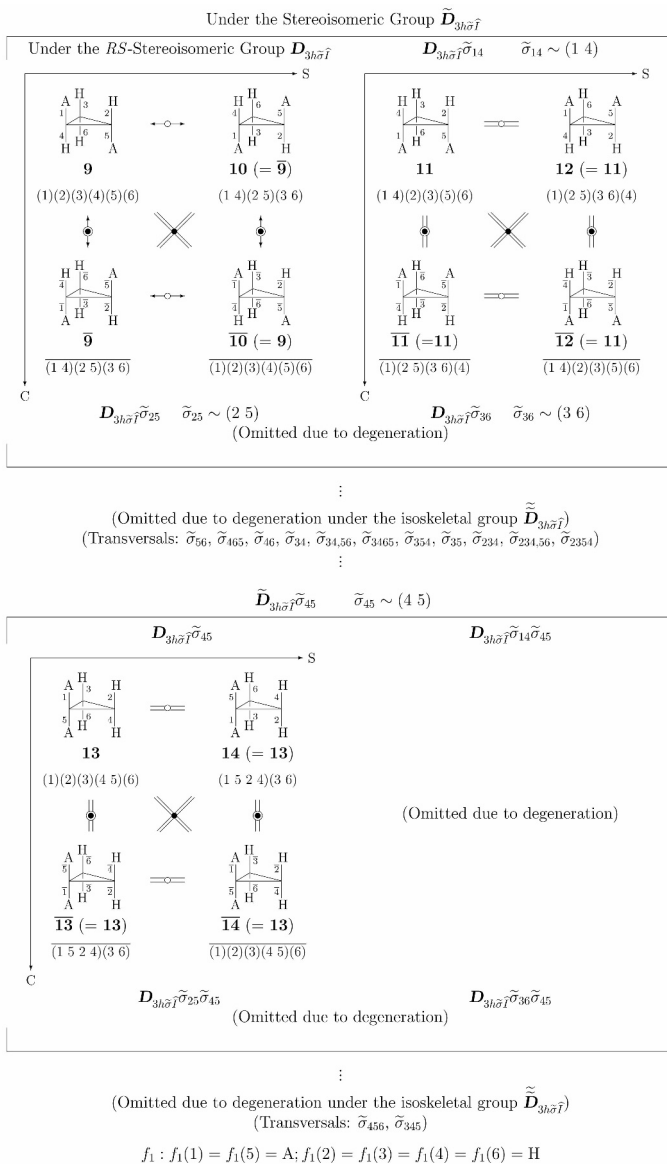


Figure 2. Hierarchy diagram for representing a multiple stereoisogram set of type $(I^2 - IV^2)^{12}/(IV^4)^3$, which is derived by putting two achiral proligands A_2 on the positions 1 and 5 of the cyclopropane skeleton **1** as well as four hydrogens H_4 on the other positions.

transversals listed in Eq. 9, two transversals, i.e., $\tilde{\sigma}_{456}$, $\tilde{\sigma}_{345}$ (in addition to the transversal $\tilde{\sigma}_{45}$) exhibits degeneration, which is summarized by the scheme $(IV^4)^3$.

Totally, the hierarchy diagram shown in Figure 2 indicates the appearance of a multiple stereoisogram set of type $(I^2 - IV^2)^{12}/(IV^4)^3$, which shows the degeneration mode of the possible 15 sets of stereoisomers ($12 + 3 = 15$) as well as the inner degeneration mode of four stereoisograms ($2 + 2 = 4$; and 4). The multiple stereoisogram set of Figure 2 is counted once under the action of isoskeletal group $\tilde{\mathbf{D}}_{3h\tilde{\sigma}\hat{\Gamma}}$, as indicated by the value 1 at the intersection between $[\hat{\theta}]_3$ -row and the $\tilde{\mathbf{D}}_{3h\tilde{\sigma}\hat{\Gamma}}$ -column in Table 4.

Under the action of the stereoisomeric group $\tilde{\mathbf{D}}_{3h\tilde{\sigma}\hat{\Gamma}}$, the two stereoisograms concerning **9** (and $\bar{\mathbf{9}}$) and **11** are equivalent and they are equalized to give one set of stereoisomers $\langle \mathbf{9} \bar{\mathbf{9}} \mathbf{11} \rangle$, where the function f_1 (Eq. 30) is applied to the numbered skeleton **1** of Figure 1. On the other hand, one stereoisogram concerning **13** (strictly speaking, a renumbered promolecule) gives one set of self-stereoisomers $\langle \mathbf{13} \rangle$ (one achiral derivative), where the following function is used:

$$f_2 : f_2(1) = f_2(4) = A; f_2(2) = f_2(3) = f_2(5) = f_2(6) = H, \quad (31)$$

which is applied to the numbered skeleton **1** of Figure 1. The application of the two functions f_1 (Eq. 30) and f_2 (Eq. 31) to **1** under the stereoisomeric group $\tilde{\mathbf{D}}_{3h\tilde{\sigma}\hat{\Gamma}}$ results in the formation of $\langle \mathbf{9} \bar{\mathbf{9}} \mathbf{11} \rangle$ (one set of stereoisomers) and $\langle \mathbf{13} \rangle$ (one set of self-stereoisomers). Thus, there appear two sets of (self-)stereoisomers, because one set of (self-)stereoisomers is counted once under the stereoisomeric group $\tilde{\mathbf{D}}_{3h\tilde{\sigma}\hat{\Gamma}}$. This is confirmed by the value 2 at the intersection between $[\hat{\theta}]_3$ -row and the $\tilde{\mathbf{D}}_{3h\tilde{\sigma}\hat{\Gamma}}$ -column in Table 4.

Under the action of the *RS*-stereoisomeric group $\mathbf{D}_{3h\tilde{\sigma}\hat{\Gamma}}$, the stereoisogram concerning $(\mathbf{9} \bar{\mathbf{9}})_I$ is inequivalent to the other stereoisogram concerning $(\mathbf{11})_{IV}$. The inequivalence between $(\mathbf{9} \bar{\mathbf{9}})_I$ and $(\mathbf{11})_{IV}$ corresponds to *cis/trans*-isomerism between them. The type-I stereoisogram concerning $(\mathbf{9} \bar{\mathbf{9}})_I$ is generated by applying the function f_1 (Eq. 30) to the $\mathbf{D}_{3h\tilde{\sigma}\hat{\Gamma}}$ -part of Figure 1, while the type-IV stereoisogram concerning $(\mathbf{11})_{IV}$ is generated by applying the following function f_3 :

$$f_3 : f_3(4) = f_3(5) = A; f_3(1) = f_3(2) = f_3(3) = f_3(6) = H \quad (32)$$

to the same $\mathbf{D}_{3h\tilde{\sigma}\hat{\Gamma}}$ -part. In addition, the type-IV stereoisogram concerning $(\mathbf{13})_{IV}$ is generated by applying the function f_2 (Eq. 31) to the same $\mathbf{D}_{3h\tilde{\sigma}\hat{\Gamma}}$ -part of Figure 1. In summary, the three stereoisograms, i.e., $(\mathbf{9} \bar{\mathbf{9}})_I$, $(\mathbf{11})_{IV}$, and $(\mathbf{13})_{IV}$, are inequivalent to

one another under the *RS*-stereoisomeric group $D_{3h\bar{\sigma}\bar{\tau}}$. This result is consistent with the value 3 at the intersection between $[\ddot{\theta}]_3$ -row and the $D_{3h\bar{\sigma}\bar{\tau}}$ -column in Table 4.

A similar discussion holds true for the action of the point group D_{3h} , so that three pairs of (self-)enantiomers, i.e., $[9\bar{9}]$, $[11]$, and $[13]$, are inequivalent under the point group D_{3h} for enantiomerism. This is consistent with the value 3 at the intersection between $[\ddot{\theta}]_3$ -row and the D_{3h} -column in Table 4. Note that the type-I stereoisogram concerning 9 contains one pair of enantiomers, i.e., $([9\bar{9}]_I)$, while the type-IV stereoisogram concerning 11 (or 13) contains one achiral promolecule, i.e. $([11]_{IV})$ (or $([13]_{IV})$).

Under the action of D_3 , the four promolecules 9 , $\bar{9}$, 11 , and 13 are determined to be inequivalent to one another, so that the value 4 at the intersection between $[\ddot{\theta}]_3$ -row and the D_3 -column in Table 4 is confirmed.

The above-mentioned steps of group hierarchy are accumulated to give the following scheme:

$$\{\langle\langle([9\bar{9}]_I) ([11]_{IV}) \langle\langle([13]_{IV})\rangle\rangle\rangle\rangle\}. \quad (33)$$

There appear equivalence classes of respective groups in Eq. 33, i.e., one pair of braces $\{\dots\}$, which contains an equivalence class of isoskeletonomers under the isoskeletal group $\tilde{D}_{3h\bar{\sigma}\bar{\tau}}$; two pairs of angle brackets $\langle\dots\rangle$, each of which contains an equivalence class of stereoisomers under the stereoisomeric group $\tilde{D}_{3h\bar{\sigma}\bar{\tau}}$; three pairs of parentheses $(\dots)_{I,IV}$, each of which contains a quadruplet of *RS*-stereoisomers as an equivalence class under the *RS*-stereoisomeric group $D_{3h\bar{\sigma}\bar{\tau}}$; three pairs of square brackets $[\dots]$, each of which contains a pair of (self-)enantiomers as an equivalence class under the point group D_{3h} ; and four promolecules without such brackets, each of which is regarded as a single-membered equivalence class under the chiral point group D_3 . Hence, the scheme of Eq. 33 is consistent with the data collected in $[\ddot{\theta}]_3$ -row of Table 4.

Such schemes as Eq. 33 is diagrammatically shown by isomer-classification diagrams, which have been proposed as convenient devices for characterizing the group hierarchy [27, 28]. Thus, the scheme represented by Eq. 33, which have been obtained the above discussions on the data of cyclopropanes with the composition H^4A^2 , can be expressed systematically by an isomer-classification diagram shown in Figure 3.

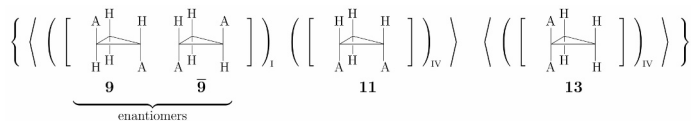


Figure 3. Isomer-classification diagram for cyclopropanes with the composition H^4A^2 . A pair of square brackets contains a pair of (self)-enantiomers, a pair of parentheses contains a quadruplet of *RS*-stereoisomers, a pair of angles contains an equivalence class of stereoisomers, and a pair of braces contains an equivalence class of isoskeletonomers.

As another set of examples of cyclopropane derivatives, the values shown in the $[\theta]_4$ -row of Table 4 can be confirmed by the isomer classification diagram shown in Figure 4, which is concerned with cyclopropanes with the composition H^4AB .

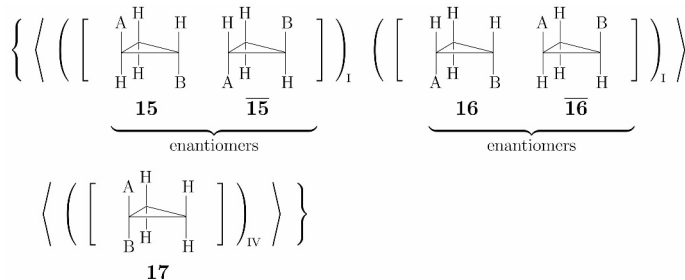


Figure 4. Isomer-classification diagram for cyclopropanes with the composition H^4AB .

Figure 4 indicates the presence of one pair of braces $\{\dots\}$, which contains an equivalence class of isoskeletonomers. Two pairs of angle brackets $\langle \dots \rangle$ indicate the presence of two equivalence classes of stereoisomers, i.e., $\langle \mathbf{15} \mathbf{15} \mathbf{16} \mathbf{16} \rangle$ and $\langle \mathbf{17} \rangle$, each of which is counted once under the stereoisomeric group $\tilde{\mathbf{D}}_{3h\sigma\hat{\tau}}$. Three pairs of parentheses $(\dots)_{\text{I,IV}}$ indicate the presence of three quadruplets of *RS*-stereoisomers, i.e., $(\mathbf{15} \mathbf{15})_{\text{I}}$, $(\mathbf{16} \mathbf{16})_{\text{I}}$, and $(\mathbf{17})_{\text{IV}}$, each of which is counted once under the *RS*-stereoisomeric group $\mathbf{D}_{3h\sigma\hat{\tau}}$. The accumulation of the results of $\tilde{\mathbf{D}}_{3h\sigma\hat{\tau}}$ and $\mathbf{D}_{3h\sigma\hat{\tau}}$ gives a partial scheme $\langle (\mathbf{15} \mathbf{15})_{\text{I}} (\mathbf{16} \mathbf{16})_{\text{I}} \rangle$, which indicates *cis/trans*-isomerism between $(\mathbf{15} \mathbf{15})_{\text{I}}$ and $(\mathbf{16} \mathbf{16})_{\text{I}}$. Three pairs of square brackets $[\dots]$ indicate the presence of three pairs of (self)-enantiomers under the point group \mathbf{D}_{3h} , where there appear two pairs of enantiomers, i.e., $[\mathbf{15} \mathbf{15}]$ and $[\mathbf{16} \mathbf{16}]$, and one pair of self-enantiomers $[\mathbf{17}]$ (one achiral promolecule). The accumulation of the results of $\tilde{\mathbf{D}}_{3h\sigma\hat{\tau}}$ and \mathbf{D}_{3h} gives another partial scheme $\langle [\mathbf{15} \mathbf{15}] [\mathbf{16} \mathbf{16}] \rangle$, which provides us with an

alternative expression of *cis/trans*-isomerism on the basis of the two pairs of enantiomers [15 15] and [16 16]. Finally, there appear five promolecules, i.e., 15, 15, 16, 16, and 17, if we do not take account of such brackets. These values are consistent with the data collected in $[\ddot{\theta}]_4$ -row of Table 4.

4.4.3 Cyclopropane derivatives with achiral and chiral proligands

Tables 5 (the partitions $[\dot{\theta}]_{12}$ - $[\dot{\theta}]_{39}$) and 6 (the partitions $[\ddot{\theta}]_{40}$ - $[\ddot{\theta}]_{55}$) collect the enumeration results of cyclopropanes with achiral and chiral proligands. Note again that the six integers at the first part of each partition are concerned with achiral proligands, while the six integers at the next part are concerned with chiral proligands (cf. Eq. 23).

As a typical example, let us examine the $[\ddot{\theta}]_{13}$ -row of Table 5, which shows the data of cyclopropanes with the composition $H^4\bar{p}^2$. Note that the composition $H^4\bar{p}^2$ corresponds to H^4p^2 , $H^4\bar{p}^2$, and $H^4p\bar{p}$ during 3D enumeration under D_3 , D_{3h} , and $D_{3h\bar{\sigma}\hat{I}}$ (cf. the set of ligand-inventory functions represented by Eqs. 18–20), while it degenerates into a single term during 2D (graph) enumeration under $\tilde{D}_{3h\bar{\sigma}\hat{I}}$ and $\tilde{D}_{3h\bar{\sigma}\hat{I}}$ (cf. the single ligand-inventory function represented by Eq. 27). The isomer-classification diagram of these cyclopropanes is shown in Figure 5.

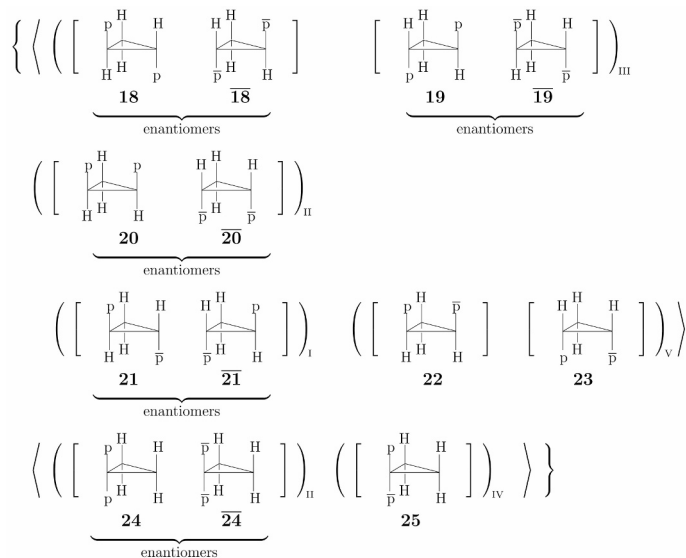


Figure 5. Isomer-classification diagram for cyclopropanes with the composition $H^4\bar{p}^2$ (H^4p^2 , $H^4\bar{p}^2$, and $H^4p\bar{p}$).

Table 5. Hierarchical Enumeration of Cyclopropane Derivatives with Achiral and Chiral Proligands (Part 1)

partition	numbers of cyclopropane derivatives				
	under respective groups				
	$T_{(D_3)\bar{\theta}}$ (Eq. 21)	$B_{(D_{3h})\bar{\theta}}$ (Eq. 24)	$B_{(D_{3h\bar{\sigma}})\bar{\theta}}$ (Eq. 25)	$B_{(\bar{D}_{3h\bar{\sigma}})\bar{\theta}}$ (Eq. 28)	$B_{(\bar{D}_{3h\bar{\sigma}})\bar{\theta}}$ (Eq. 29)
	Eq. 18-20			Eq. 27	
$[\hat{\theta}]_{12} = [5, 0, 0, 0, 0, 0, 1, 0, 0, 0, 0, 0]$	2	1	1	1	1
$[\hat{\theta}]_{13} = [4, 0, 0, 0, 0, 0, 2, 0, 0, 0, 0, 0]$	13	8	6	2	1
$[\hat{\theta}]_{14} = [4, 1, 0, 0, 0, 0, 1, 0, 0, 0, 0, 0]$	10	5	3	2	1
$[\hat{\theta}]_{15} = [4, 0, 0, 0, 0, 0, 1, 1, 0, 0, 0, 0]$	20	10	6	2	1
$[\hat{\theta}]_{16} = [3, 0, 0, 0, 0, 0, 3, 0, 0, 0, 0, 0]$	28	14	9	2	1
$[\hat{\theta}]_{17} = [3, 2, 0, 0, 0, 0, 1, 0, 0, 0, 0, 0]$	20	10	6	3	1
$[\hat{\theta}]_{18} = [3, 1, 0, 0, 0, 0, 2, 0, 0, 0, 0, 0]$	40	22	12	3	1
$[\hat{\theta}]_{19} = [3, 0, 0, 0, 0, 0, 2, 1, 0, 0, 0, 0]$	80	40	22	3	1
$[\hat{\theta}]_{20} = [3, 1, 1, 0, 0, 0, 1, 0, 0, 0, 0, 0]$	40	20	10	4	1
$[\hat{\theta}]_{21} = [3, 1, 0, 0, 0, 0, 1, 1, 0, 0, 0, 0]$	80	40	20	4	1
$[\hat{\theta}]_{22} = [3, 0, 0, 0, 0, 0, 1, 1, 1, 0, 0, 0]$	160	80	40	4	1
$[\hat{\theta}]_{23} = [2, 2, 0, 0, 0, 0, 2, 0, 0, 0, 0, 0]$	66	36	22	5	1
$[\hat{\theta}]_{24} = [2, 0, 0, 0, 0, 0, 2, 2, 0, 0, 0, 0]$	252	130	74	5	1
$[\hat{\theta}]_{25} = [2, 2, 1, 0, 0, 0, 1, 0, 0, 0, 0, 0]$	60	30	16	6	1
$[\hat{\theta}]_{26} = [2, 2, 0, 0, 0, 0, 1, 1, 0, 0, 0, 0]$	120	60	32	6	1
$[\hat{\theta}]_{27} = [2, 0, 0, 0, 0, 0, 2, 1, 1, 0, 0, 0]$	480	240	124	6	1
$[\hat{\theta}]_{28} = [2, 1, 1, 0, 0, 0, 2, 0, 0, 0, 0, 0]$	120	62	32	6	1
$[\hat{\theta}]_{29} = [2, 1, 0, 0, 0, 0, 2, 1, 0, 0, 0, 0]$	240	120	62	6	1
$[\hat{\theta}]_{30} = [2, 1, 1, 1, 0, 0, 1, 0, 0, 0, 0, 0]$	120	60	30	9	1
$[\hat{\theta}]_{31} = [2, 1, 1, 0, 0, 0, 1, 1, 0, 0, 0, 0]$	240	120	60	9	1
$[\hat{\theta}]_{32} = [2, 1, 0, 0, 0, 0, 1, 1, 1, 0, 0, 0]$	480	240	120	9	1
$[\hat{\theta}]_{33} = [2, 0, 0, 0, 0, 0, 1, 1, 1, 1, 0, 0]$	960	480	240	9	1
$[\hat{\theta}]_{34} = [1, 1, 1, 1, 1, 1, 0, 0, 0, 0, 0, 0]$	120	60	60	15	1
$[\hat{\theta}]_{35} = [1, 1, 1, 1, 1, 0, 1, 0, 0, 0, 0, 0]$	240	120	60	15	1
$[\hat{\theta}]_{36} = [1, 1, 1, 1, 0, 0, 1, 1, 0, 0, 0, 0]$	480	240	120	15	1
$[\hat{\theta}]_{37} = [1, 1, 1, 0, 0, 0, 1, 1, 1, 0, 0, 0]$	960	480	240	15	1
$[\hat{\theta}]_{38} = [1, 1, 0, 0, 0, 0, 1, 1, 1, 1, 0, 0]$	1920	960	480	15	1
$[\hat{\theta}]_{39} = [1, 0, 0, 0, 0, 0, 1, 1, 1, 1, 1, 0]$	3840	1920	960	15	1

Table 6. Hierarchical Enumeration of Cyclopropane Derivatives with Achiral and Chiral Proligands (Part 2)

partition	numbers of cyclopropane derivatives under respective groups				
	$T_{(D_3)\bar{\theta}}$	$B_{(D_{3h})\bar{\theta}}$	$B_{(D_{3h\bar{\sigma}})\bar{\theta}}$	$B_{(\bar{D}_{3h\bar{\sigma}})\bar{\theta}}$	$B_{(\tilde{D}_{3h\bar{\sigma}})\bar{\theta}}$
	(Eq. 21)	(Eq. 24)	(Eq. 25)	(Eq. 28)	(Eq. 29)
	Eqs. 18–20			Eq. 27	
$[\hat{\theta}]_{40} = [1, 0, 0, 0, 0, 0, 5, 0, 0, 0, 0, 0]$	32	16	10	1	1
$[\hat{\theta}]_{41} = [2, 0, 0, 0, 0, 0, 4, 0, 0, 0, 0, 0]$	46	25	17	2	1
$[\hat{\theta}]_{42} = [1, 0, 0, 0, 0, 0, 4, 1, 0, 0, 0, 0]$	160	80	42	2	1
$[\hat{\theta}]_{43} = [1, 1, 0, 0, 0, 0, 4, 0, 0, 0, 0, 0]$	80	42	22	2	1
$[\hat{\theta}]_{44} = [1, 0, 0, 0, 0, 0, 3, 2, 0, 0, 0, 0]$	320	160	84	3	1
$[\hat{\theta}]_{45} = [2, 0, 0, 0, 0, 0, 3, 1, 0, 0, 0, 0]$	160	80	44	3	1
$[\hat{\theta}]_{46} = [2, 1, 0, 0, 0, 0, 3, 0, 0, 0, 0, 0]$	80	40	22	3	1
$[\hat{\theta}]_{47} = [1, 0, 0, 0, 0, 0, 3, 1, 1, 0, 0, 0]$	640	320	160	4	1
$[\hat{\theta}]_{48} = [1, 1, 0, 0, 0, 0, 3, 1, 0, 0, 0, 0]$	320	160	80	4	1
$[\hat{\theta}]_{49} = [1, 1, 1, 0, 0, 0, 3, 0, 0, 0, 0, 0]$	160	80	40	4	1
$[\hat{\theta}]_{50} = [1, 0, 0, 0, 0, 0, 2, 2, 1, 0, 0, 0]$	960	480	244	6	1
$[\hat{\theta}]_{51} = [1, 1, 0, 0, 0, 0, 2, 2, 0, 0, 0, 0]$	480	244	124	6	1
$[\hat{\theta}]_{52} = [1, 0, 0, 0, 0, 0, 2, 1, 1, 1, 0, 0]$	1920	960	480	9	1
$[\hat{\theta}]_{53} = [1, 1, 0, 0, 0, 0, 2, 1, 1, 0, 0, 0]$	960	480	240	9	1
$[\hat{\theta}]_{54} = [1, 1, 1, 0, 0, 0, 2, 1, 0, 0, 0, 0]$	480	240	120	9	1
$[\hat{\theta}]_{55} = [1, 1, 1, 1, 0, 0, 2, 0, 0, 0, 0, 0]$	240	120	60	9	1

Figure 5 is consistent with the data collected in the $[\hat{\theta}]_{13}$ -row of Table 5. Thus, Figure 5 indicates the presence of one pair of braces $\{\cdot\cdot\}$, which contains an equivalence class of isoskeletomers. These isoskeletomers are equivalent to each other under the action of the isoskeletal group $\tilde{\tilde{D}}_{3h\bar{\sigma}\hat{\tau}}$. Because the equivalence class of isoskeletomers is totally counted once under $\tilde{\tilde{D}}_{3h\bar{\sigma}\hat{\tau}}$, this itemization by a single pair of braces is verified by the value 1 at the $B_{(\tilde{D}_{3h\bar{\sigma}})\bar{\theta}}$ -column.

Two pairs of angle brackets $\langle\cdot\cdot\rangle$ in Figure 5 indicate the presence of two sets of stereoisomers, i.e., $\langle\mathbf{18} \overline{\mathbf{18}} \mathbf{19} \overline{\mathbf{19}} \mathbf{20} \overline{\mathbf{20}} \mathbf{21} \overline{\mathbf{21}} \mathbf{22} \mathbf{23}\rangle$ and $\langle\mathbf{24} \overline{\mathbf{24}} \mathbf{25}\rangle$, each of which is counted once under the action of the stereoisomeric group $\tilde{\tilde{D}}_{3h\bar{\sigma}\hat{\tau}}$. This is consistent with the value 2 at the intersection between the $[\hat{\theta}]_{13}$ -row and the $B_{(\tilde{D}_{3h\bar{\sigma}})\bar{\theta}}$ -column.

Six pairs of parentheses $(\cdot\cdot)_{I-V}$ in Figure 5 indicate the presence of six sets of *RS*-stereoisomers, i.e., $(\mathbf{18} \overline{\mathbf{18}} \mathbf{19} \overline{\mathbf{19}})_{III}$, $(\mathbf{20} \overline{\mathbf{20}})_{II}$, $(\mathbf{21} \overline{\mathbf{21}})_{I}$, $(\mathbf{22} \mathbf{23})_{V}$, $(\mathbf{24} \overline{\mathbf{24}})_{II}$, and $(\mathbf{25})_{IV}$, each of which is counted once under the action of the *RS*-stereoisomeric group

$\mathbf{D}_{3h\bar{\sigma}\bar{\tau}}$. This is consistent with the value 6 at the intersection with the $B_{(\mathbf{D}_{3h\bar{\sigma}\bar{\tau}})\bar{\theta}}$ -column.

Eight pairs of square brackets $[\dots]$ in Figure 5 indicate the presence of eight pairs of (self)-enantiomers, i.e., [18 $\bar{18}$], [19 $\bar{19}$], [20 $\bar{20}$][21 $\bar{21}$], [22], [23], [24 $\bar{24}$], and [25], each of which is counted once under the action of the point group \mathbf{D}_{3h} . The number 8 is consistent with the value 8 appearing at the intersection between the $[\bar{\theta}]_{13}$ -row and the $B_{(\mathbf{D}_{3h})\bar{\theta}}$ -column in Table 5. The expression (*self*-)enantiomers is used because there appear five pairs of enantiomers and three pairs of self-enantiomers (i.e., three achiral promolecules).

Finally, there appear 13 promolecules in Figure 5, if we do not take account of such brackets. They are inequivalent under the point group \mathbf{D}_3 . Because each of them is counted once under \mathbf{D}_3 , the number 13 is consistent with the value 13 appearing at the intersection between the $[\bar{\theta}]_{13}$ -row and the $T_{(\mathbf{D}_3)\bar{\theta}}$ -column in Table 5.

It should be again noted that the composition $\text{H}^4\bar{\text{p}}^2$ for the partition $[\bar{\theta}]_{13}$ is itemized into H^4p^2 , $\text{H}^4\bar{\text{p}}^2$, and $\text{H}^4\text{p}\bar{\text{p}}$. To draw such isomer-classification diagram as Figure 5 systematically, the itemization concerning p and $\bar{\text{p}}$ is desirable in the enumeration of pairs of enantiomers (the eight pairs of square brackets $[\dots]$) under the point group \mathbf{D}_{3h} . For this purpose, the ligand inventory $\mathbf{L}_{3\text{D}}$ (Eq. 14) is restricted to $\mathbf{L}'_{3\text{D}} = \{\text{H}, \text{p}, \bar{\text{p}}\}$. Thereby, Eqs. 15–17 are restricted to give the following ligand-inventory functions:

$$a_d = \text{H}^d \quad (34)$$

$$c_d = \text{H}^d + 2\text{p}^{d/2}\bar{\text{p}}^{d/2} \quad (35)$$

$$b_d = \text{H}^d + \text{p}^d + \bar{\text{p}}^d. \quad (36)$$

These ligand-inventory functions are introduced into the CI-CF of the point group \mathbf{D}_{3h} (Eq. 13). The expansion of the resulting equation generates the following generating function:

$$\begin{aligned} \sum_{\theta} B'_{(\mathbf{D}_{3h})\bar{\theta}} W_{\bar{\theta}} &= \text{CI-CF}(\mathbf{D}_{3h}, \mathbb{S}_d) \Big|_{\text{Eqs. 34-36}} \\ &= \text{H}^6 + \frac{1}{2}(\text{H}^5\text{p} + \text{H}^5\bar{\text{p}}) \\ &+ 4 \times \frac{1}{2}(\text{H}^4\text{p}^2 + \text{H}^4\bar{\text{p}}^2) + 4\text{H}^4\text{p}\bar{\text{p}} \\ &+ 4 \times \frac{1}{2}(\text{H}^3\text{p}^3 + \text{H}^3\bar{\text{p}}^3) + 10 \times \frac{1}{2}(\text{H}^3\text{p}^2\bar{\text{p}} + \text{H}^3\text{p}\bar{\text{p}}^2) \\ &+ 4 \times \frac{1}{2}(\text{H}^2\text{p}^4 + \text{H}^2\bar{\text{p}}^4) + 10 \times \frac{1}{2}(\text{H}^2\text{p}^3\bar{\text{p}} + \text{H}^2\text{p}\bar{\text{p}}^3) + 11\text{H}^2\text{p}^2\bar{\text{p}}^2 \end{aligned}$$

$$\begin{aligned}
 & + \frac{1}{2}(\text{Hp}^5 + \text{H}\bar{\text{p}}^5) + 5 \times \frac{1}{2}(\text{Hp}^4\bar{\text{p}} + \text{Hp}\bar{\text{p}}^4) + 10 \times \frac{1}{2}(\text{Hp}^3\bar{\text{p}}^2 + \text{Hp}^2\bar{\text{p}}^3) \\
 & + \frac{1}{2}(\text{p}^6 + \bar{\text{p}}^6) + \frac{1}{2}(\text{p}^5\bar{\text{p}} + \text{p}\bar{\text{p}}^5) + 4 \times \frac{1}{2}(\text{p}^4\bar{\text{p}}^2 + \text{p}^2\bar{\text{p}}^4) + 3\text{p}^3\bar{\text{p}}^3. \quad (37)
 \end{aligned}$$

Among the terms appearing in Eq. 37, the terms $4 \times \frac{1}{2}(\text{H}^4\text{p}^2 + \text{H}^4\bar{\text{p}}^2)$ and $\text{H}^4\text{p}\bar{\text{p}}$ correspond to the composition $\text{H}^4\bar{\text{p}}^2$. Because the combined term $\frac{1}{2}(\text{H}^4\text{p}^2 + \text{H}^4\bar{\text{p}}^2)$ corresponds to a pair of enantiomers with the composition H^4p^2 (or $\text{H}^4\bar{\text{p}}^2$), the coefficient 4 of this combined term indicates the presence of four pairs of enantiomers, i.e., [18 18], [19 19], [20 20], and [24 24]. On the other hand, the term $\text{H}^4\text{p}\bar{\text{p}}$ corresponds to a pair of (self-)enantiomers with composition $\text{H}^4\text{p}\bar{\text{p}}$. It follows that the coefficient 4 of this term indicates the presence of four pairs of (self-)enantiomers, which are found to be one pair of enantiomers [21 21] and three achiral cyclopropanes [22], [23], and [25].

4.4.4 Cyclopropane derivatives with chiral proligands

Table 7 collects the enumeration results of cyclopropanes with chiral proligands and no achiral proligands, where the partitions $[\check{\theta}]_{56} - [\check{\theta}]_{66}$ are taken into consideration.

Table 7. Hierarchical Enumeration of Cyclopropane Derivatives with Chiral Proligands and No Achiral Proligands

partition	numbers of cyclopropane derivatives under respective groups				
	$T_{(\text{D}_3)\check{\theta}}$	$B_{(\text{D}_{3h})\check{\theta}}$	$B_{(\text{D}_{3h\bar{\sigma}})\check{\theta}}$	$B_{(\bar{\text{D}}_{3h\bar{\sigma}})\check{\theta}}$	$B_{(\bar{\text{D}}_{3h\bar{\sigma}})\check{\theta}}$
	(Eq. 21)	(Eq. 24)	(Eq. 25)	(Eq. 28)	(Eq. 29)
	Eqs. 18-20			Eq. 27	
$[\check{\theta}]_{56} = [0, 0, 0, 0, 0, 0, 6, 0, 0, 0, 0, 0]$	16	9	8	1	1
$[\check{\theta}]_{57} = [0, 0, 0, 0, 0, 0, 5, 1, 0, 0, 0, 0]$	64	32	20	1	1
$[\check{\theta}]_{58} = [0, 0, 0, 0, 0, 0, 4, 2, 0, 0, 0, 0]$	172	88	54	2	1
$[\check{\theta}]_{59} = [0, 0, 0, 0, 0, 0, 4, 1, 1, 0, 0, 0]$	320	160	84	2	1
$[\check{\theta}]_{60} = [0, 0, 0, 0, 0, 0, 3, 3, 0, 0, 0, 0]$	216	108	62	2	1
$[\check{\theta}]_{61} = [0, 0, 0, 0, 0, 0, 3, 2, 1, 0, 0, 0]$	640	320	168	3	1
$[\check{\theta}]_{62} = [0, 0, 0, 0, 0, 0, 3, 1, 1, 1, 0, 0]$	1280	640	320	4	1
$[\check{\theta}]_{63} = [0, 0, 0, 0, 0, 0, 2, 2, 2, 0, 0, 0]$	984	496	268	5	1
$[\check{\theta}]_{64} = [0, 0, 0, 0, 0, 0, 2, 2, 1, 1, 0, 0]$	1920	960	488	6	1
$[\check{\theta}]_{65} = [0, 0, 0, 0, 0, 0, 2, 1, 1, 1, 1, 0]$	3840	1920	960	9	1
$[\check{\theta}]_{66} = [0, 0, 0, 0, 0, 0, 1, 1, 1, 1, 1, 1]$	7680	3840	1920	15	1

As a typical example for illustrating the enumeration results of Table 7, let us examine its $[\check{\theta}]_{56}$ -row, which shows the data of cyclopropanes with the composition $\check{\text{p}}^6$ ($\text{p}^6/\bar{\text{p}}^6$,

$p^5\bar{p}/p\bar{p}^5$, $p^4\bar{p}^2/p^2\bar{p}^4$, and $p^3\bar{p}^3$). The isomer-classification diagram of these cyclopropanes is shown in Figure 6, which is consistent with the data collected in the $[\check{\theta}]_{56}$ -row of Table 7.

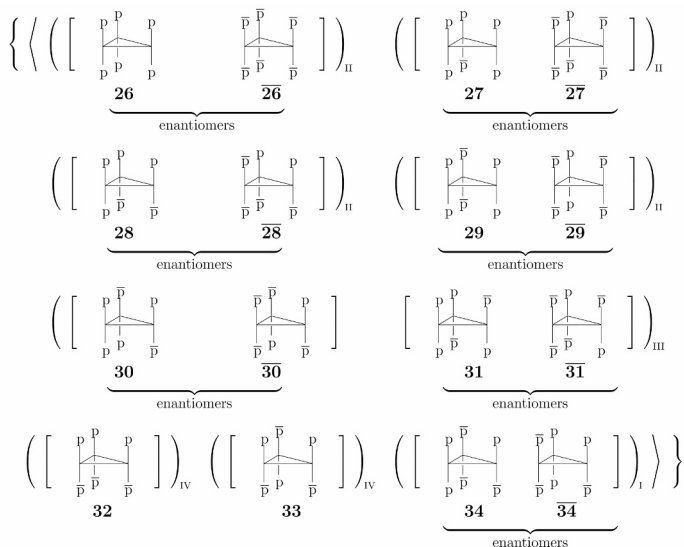


Figure 6. Isomer-classification diagram for cyclopropanes with the composition \check{p}^6 (p^6/\bar{p}^6 , $p^5\bar{p}/p\bar{p}^5$, $p^4\bar{p}^2/p^2\bar{p}^4$, and $p^3\bar{p}^3$).

Figure 6 indicates the presence of an equivalence class of isoskeletons, as surrounded by a pair of braces $\{\dots\}$. Because the equivalence class of isoskeletons is counted once under the isoskeletal group $\tilde{\tilde{D}}_{3h\bar{\sigma}\bar{\tau}}$, the value 1 at the intersection between the $[\check{\theta}]_{56}$ -row and the $B_{(\tilde{\tilde{D}}_{3h\bar{\sigma}\bar{\tau}})^{\check{\theta}}}$ -column is verified diagrammatically.

One pair of angle brackets $\langle \dots \rangle$ in Figure 6 indicates the presence of one set of stereoisomers, which is counted once under the action of the stereoisomeric group $\tilde{D}_{3h\bar{\sigma}\bar{\tau}}$. This is consistent with the value 1 at the intersection between the $[\check{\theta}]_{56}$ -row and the $B_{(\tilde{D}_{3h\bar{\sigma}\bar{\tau}})^{\check{\theta}}}$ -column.

Eight pairs of parentheses $(\dots)_{\text{I-IV}}$ in Figure 6 indicate the presence of eight quadruplets of *RS*-stereoisomers, i.e., $(26 \bar{26})_{\text{II}}$, $(27 \bar{27})_{\text{II}}$, $(28 \bar{28})_{\text{II}}$, $(29 \bar{29})_{\text{II}}$, $(30 \bar{30} \ 31 \ \bar{31})_{\text{III}}$, $(32)_{\text{IV}}$, $(33)_{\text{IV}}$, and $(34 \ \bar{34})_{\text{I}}$, each of which is counted once under the action of the *RS*-stereoisomeric group $D_{3h\bar{\sigma}\bar{\tau}}$. This is consistent with the value 8 at the intersection between the $[\check{\theta}]_{56}$ -row and the $B_{(D_{3h\bar{\sigma}\bar{\tau}})^{\check{\theta}}}$ -column.

Nine pairs of square brackets $[\dots]$ in Figure 6 indicate the presence of nine pairs of (self)-enantiomers, i.e., $[26 \overline{26}]$, $[27 \overline{27}]$, $[28 \overline{28}]$, $[29 \overline{29}]$, $[30 \overline{30}]$, $[31 \overline{31}]$, $[32]$, $[33]$, and $[34 \overline{34}]$, each of which is counted once under the action of the point group D_{3h} . The number 9 is consistent with the value 9 appearing at the intersection between the $[\tilde{\theta}]_{56}$ -row and the $B_{(D_{3h})\tilde{\theta}}$ -column in Table 5.

Finally, there appear 16 promolecules in Figure 6, if we do not take account of such brackets. They are inequivalent under the point group D_3 . Because each of them is counted once under D_3 , the number 16 is consistent with the value 16 appearing at the intersection between the $[\tilde{\theta}]_{56}$ -row and the $T_{(D_3)\tilde{\theta}}$ -column in Table 5.

The partition $[\tilde{\theta}]_{56}(\tilde{p}^6)$ is itemized into p^6/\overline{p}^6 , $p^5\overline{p}/p\overline{p}^5$, $p^4\overline{p}^2/p^2\overline{p}^4$, and $p^3\overline{p}^3$. The effect of this itemization is evaluated by the last row of Eq. 37. The term $\frac{1}{2}(p^6 + \overline{p}^6)$ indicates the presence of one pair of enantiomers with the composition p^6/\overline{p}^6 , i.e., $[26 \overline{26}]$. The term $\frac{1}{2}(p^5\overline{p} + p\overline{p}^5)$ indicates the presence of one pair of enantiomers with the composition $p^5\overline{p}/p\overline{p}^5$, i.e., $[27 \overline{27}]$. The term $4 \times \frac{1}{2}(p^4\overline{p}^2 + p^2\overline{p}^4)$ indicates the presence of four pairs of enantiomers with the composition $p^4\overline{p}^2/p^2\overline{p}^4$, i.e., $[28 \overline{28}]$, $[29 \overline{29}]$, $[30 \overline{30}]$, and $[31 \overline{31}]$. The term $3p^3\overline{p}^3$ of Eq. 37 indicates the presence of three pairs of (self)-enantiomers with the composition $p^3\overline{p}^3$, i.e., $[32]$, $[33]$, and $[34 \overline{34}]$.

4.4.5 Pólya's enumeration method as a special case of the present approach

The use of the single ligand-inventory function (Eq. 27) results in the degeneration of the stereoisomeric group $\tilde{D}_{3h\tilde{\sigma}\tilde{\tau}}$ (Eq. 8) into the following group:

$$\tilde{D}_{3\tilde{\sigma}} = D_{3\tilde{\sigma}} + D_{3\tilde{\sigma}}\tilde{\sigma}_{14} + D_{3\tilde{\sigma}}\tilde{\sigma}_{25} + D_{3\tilde{\sigma}}\tilde{\sigma}_{36}, \quad (38)$$

which consists of permutations without reflections. Note that the RS -permutation group $D_{3\tilde{\sigma}}$ (Eq. 4) is used to generate the coset decomposition of $\tilde{D}_{3\tilde{\sigma}}$ (Eq. 38) by adopting the same set of transversals contained in Eq. 8. The order of $\tilde{D}_{3\tilde{\sigma}}$ is calculated to be 48, which is a half of the order 96 of $\tilde{D}_{3h\tilde{\sigma}\tilde{\tau}}$. The generator set $cD3s$ of the $\tilde{D}_{3\tilde{\sigma}}$ is obtained by omitting the permutation (7,8) from the generator set of $\tilde{D}_{3h\tilde{\sigma}\tilde{\tau}}$ ($cD3hsI$ shown in Table 3). Thereby, the corresponding CI-CF (CI-CF($\tilde{D}_{3\tilde{\sigma}}, b_d$)) denoted by the symbol $CICF_cD3s$ is obtained as follows:

```
gap> Read("c:/fujita0/fujita2017/D3hsI-GAP/calcc-GAP/CICFgenCC.gapfunc");
gap> cD3s := Group([(3,6), (2,3)(5,6), (1,2)(4,5)]);
Group([(3,6), (2,3)(5,6), (1,2)(4,5)])
gap> CICF_cD3s := CalcConjClassCICF(cD3s, 6, 6);
1/48*b_1^6+1/16*b_1^4*b_2+3/16*b_1^2*b_2^2+1/8*b_1^2*b_4+7/48*b_2^3+1/8*b_2*b_4+1/6*b_3^2+1/6*b_6
```

By introducing Eq. 27 into the CI-CF (CICF_cD3s), we obtain the following generating function:

$$\sum_{\tilde{\theta}} B_{(\tilde{D}_{3\tilde{\sigma}})\tilde{\theta}} W_{\tilde{\theta}} = \text{CI-CF}(\tilde{D}_{3\tilde{\sigma}}, b_d) \Big|_{\text{Eq. 27}}. \quad (39)$$

Because of the degenerate nature from Eq. 8 to Eq. 38, the comparison between Eq. 28 and Eq. 39 results in the equality between $B_{(\tilde{D}_{3h\tilde{\sigma}\tilde{\tau}})\tilde{\theta}} = B_{(\tilde{D}_{3\tilde{\sigma}})\tilde{\theta}}$ with respect to the coefficients of $W_{\tilde{\theta}}$.

Note that the single ligand-inventory function (Eq. 27) for stereoisomer enumeration (2D enumeration) is regarded as degenerating into b_d , as found in the resulting CICF_cD3s. Strictly speaking, the sphericity index b_d requires Eq. 17 or Eq. 20, if we aims at 3D enumeration.

For the purpose of using Pólya's enumeration method [29,30], the cyclopropane skeleton **1** as a 3D structure is converted into another skeleton **1_g** as a graph (a 2D structure), as shown in Figure 7. The six positions of **1_g** are controlled by the permutation group isomorphic to $\tilde{D}_{3\tilde{\sigma}}$ (Eq. 38). Note, however, that the epimerization operations $\tilde{\sigma}_{14}$, $\tilde{\sigma}_{25}$, and $\tilde{\sigma}_{36}$ for characterizing the epimerizations of **1** (3D operations) are now regarded as permutations of **1_g** (2D operations) and that such a reflection as $\sigma_h \sim \overline{(1\ 4)(2\ 5)(3\ 6)}$ (as an element of the point group D_{3h}) for the 3D skeleton **1** is replaced by such a permutation as $\tilde{\sigma}_h \sim (1\ 4)(2\ 5)(3\ 6)$ (as an element of the *RS*-permutation group $D_{3\tilde{\sigma}}$) in the case of the graph **1_g**.

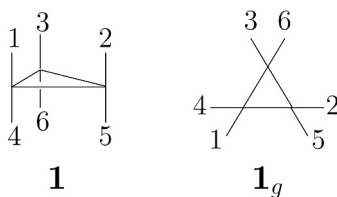


Figure 7. Cyclopropane skeletons as a 3D structure and as a graph (2D structure)

Because the function `CycleIndex` is equipped originally in the GAP system, the Pólya's cycle index (CI($\tilde{D}_{3\tilde{\sigma}}, x_d$)) denoted by the symbol `CI_cD3s` is obtained as follows:

```
gap> cD3s := Group([(3,6), (2,3)(5,6), (1,2)(4,5)]);
Group([(3,6), (2,3)(5,6), (1,2)(4,5)])
gap> CI_cD3s := CycleIndex(cD3s);
1/48*x_1^6+1/16*x_1^4*x_2+3/16*x_1^2*x_2^2+1/8*x_1^2*x_4+7/48*x_2^3+1/8*x_2*x_4+1/6*x_3^2+1/6*x_6
```

Pólya used the concept of coronas (wreath products) to treat the graph **1_g** under the title *topological interpretations* in Section 56 of [29,30]. Thus, the triangular skeleton of **1_g**

is regarded as being controlled by the symmetric group of degree 3 ($\mathbf{S}^{[3]}$, $\mathbf{S3}$) and each of the methylene units (1-C-4, 2-C-5, and 3-C-6 units) is regarded as being controlled by the symmetric group of degree 2 ($\mathbf{S}^{[2]}$, $\mathbf{S2}$). Thereby, the graph $\mathbf{1}_g$ is totally controlled by the corona ($\mathbf{S}^{[3]}[\mathbf{S}^{[2]}]$, $\mathbf{S2S3}$), which gives the corresponding cycle index ($\text{CI}(\mathbf{S}^{[3]}[\mathbf{S}^{[2]}], x_d)$) (cf. Eq. 3.1 of [29,30]). The equivalence between Pólya's treatment (Section 56 of [29,30]) and the degenerate case of the present approach is confirmed by the GAP system, where the isomorphism between $\tilde{\mathbf{D}}_{3\bar{\sigma}}$ ($\mathbf{cD3s}$) and $\mathbf{S}^{[3]}[\mathbf{S}^{[2]}]$ ($\mathbf{S2S3}$) is shown by using the GAP function `IsomorphismGroups` as follows:

```
gap> cD3s := Group([(3,6), (2,3)(5,6), (1,2)(4,5)]);
gap> S3 := Group([(1,2,3), (1,2)]);
gap> S2 := Group([(1,2)]);
gap> S2S3 := WreathProduct(S2, S3);
Group([ (1,2), (3,4), (5,6), (1,3,5)(2,4,6), (1,3)(2,4) ])
gap> IsomorphismGroups(cD3s,S2S3);
[ (3,6), (2,3)(5,6), (1,2)(4,5) ] -> [ (1,2), (1,3)(2,4), (3,5)(4,6) ]
gap> CI_S2S3 := CycleIndex(S2S3);
1/48*x_1^6+1/16*x_1^4*x_2+3/16*x_1^2*x_2^2+1/8*x_1^2*x_4+7/48*x_2^3+1/8*x_2*x_4+1/6*x_3^2+1/6*x_6
```

The resulting CI (`CI_S2S3`) obtained by `CycleIndex(S2S3)` is identical with the above CI (`CI_cD3s`) obtained by `CycleIndex(cD3s)`.

For the purpose of calculating a generating function, we use the following inventory function:

$$x_d = H^d + A^d + B^d + C^d + D^d + V^d + \check{p}^d + \check{q}^d + \check{r}^d + \check{s}^d + \check{t}^d + \check{u}^d, \quad (40)$$

which is obtained by placing $x_d = a_d = c_d = b_d$ in Eq. 27. By introducing Eq. 40 into the CI (`CI_cD3s` or `CI_S2S3`), we obtain the following generating function:

$$\sum_{\check{\theta}} B'_{(\tilde{\mathbf{D}}_{3\bar{\sigma}})\check{\theta}} W_{\check{\theta}} = \text{CI}(\tilde{\mathbf{D}}_{3\bar{\sigma}}, x_d) \Big|_{\text{Eq. 40}}. \quad (41)$$

If we place $b_d = x_d$, the CI for $\tilde{\mathbf{D}}_{3\bar{\sigma}}$ ($\text{CI}(\tilde{\mathbf{D}}_{3\bar{\sigma}}, x_d)$, `CI_cD3s`) in Eq. 41 is formally identical with the CI-CF for $\tilde{\mathbf{D}}_{3\bar{\sigma}}$ ($\text{CI-CF}(\tilde{\mathbf{D}}_{3\bar{\sigma}}, b_d)$, `CICF_cD3s`) in Eq. 28. Hence, Eq. 39 (for 3D structures) and Eq. 41 (for graphs) are formally equal to each other, so long as Eq. 27 for b_d as a single ligand-inventory function is equal to Eq. 40 for x_d . Hence, the coefficient $B_{(\tilde{\mathbf{D}}_{3\bar{\sigma}})\check{\theta}}$ of the composition $W_{\check{\theta}}$ in Eq. 39 is equal to the coefficient $B'_{(\tilde{\mathbf{D}}_{3\bar{\sigma}})\check{\theta}}$ of $W_{\check{\theta}}$ in Eq. 41. In summary, we obtain $B'_{(\tilde{\mathbf{D}}_{3\bar{\sigma}})\check{\theta}} = B_{(\tilde{\mathbf{D}}_{3\bar{\sigma}})\check{\theta}} = B_{(\tilde{\mathbf{D}}_{3h\bar{\sigma}\hat{\Gamma}})\check{\theta}}$ with respect to the coefficients of $W_{\check{\theta}}$. As a result, Pólya's enumeration method based on the CI for $\tilde{\mathbf{D}}_{3\bar{\sigma}}$ ($\text{CI}(\tilde{\mathbf{D}}_{3\bar{\sigma}}, x_d)$, `CI_cD3s`) is concluded to be a special case of Fujita's proligand method based on the CI-CF for $\tilde{\mathbf{D}}_{3h\bar{\sigma}\hat{\Gamma}}$ ($\text{CI-CF}(\tilde{\mathbf{D}}_{3h\bar{\sigma}\hat{\Gamma}}, \$d)$, `CICF_cD3hsI`) via the CI-CF for $\tilde{\mathbf{D}}_{3\bar{\sigma}}$ ($\text{CI-CF}(\tilde{\mathbf{D}}_{3\bar{\sigma}}, b_d)$, `CICF_cD3s`). The discussions described above show that this conclusion holds true in general.

5 Conclusion

Group hierarchy for characterizing a cyclopropane skeleton with six substitution positions has been discussed by defining the point group D_{3h} (order 12) for enantiomerism, the *RS*-stereoisomeric group $D_{3h\bar{\sigma}\hat{\Gamma}}$ (order 24) for *RS*-stereoisomerism, the stereoisomeric group $\tilde{D}_{3h\bar{\sigma}\hat{\Gamma}}$ (order 96) for stereoisomerism, and the isoskeletal group $\tilde{\tilde{D}}_{3h\bar{\sigma}\hat{\Gamma}}$ (order 1440) for isoskeletomerism. These groups are constructed successively by starting from the point group D_3 , where each group is defined by the coset decomposition concerning its subgroup. They are generated as the corresponding combined-permutation representations of degree 8 based on respective sets of generators, where permutation representations of degree 6 are combined with the mirror-permutation representations of degree 2. Thereby, hierarchical enumeration of cyclopropane derivatives is conducted by calculating cycle indices with chirality fittingness (CI-CFs), which consists of sphericity indices (SIs) a_d , c_d , and b_d . For the purpose of enumerating cyclopropane derivatives under the point groups D_3 and D_{3h} as well as under the *RS*-stereoisomeric group $D_{3h\bar{\sigma}\hat{\Gamma}}$, a set of three ligand-inventory functions for SIs is defined to accomplish 3D enumerations. For the purpose of 2D-based enumerations under the stereoisomeric group $\tilde{D}_{3h\bar{\sigma}\hat{\Gamma}}$ and under the isoskeletal group $\tilde{\tilde{D}}_{3h\bar{\sigma}\hat{\Gamma}}$, a single ligand-inventory function is used in accord with the degeneration of the SIs ($a_d = c_d = b_d$). The enumeration results are discussed systematically in terms of isomer-classification diagrams.

Appendix A. Source list of `enumD3hsI-stsk.gap` for enumerating cyclopropane derivatives

The following program for combinatorial enumeration of cyclopropane derivatives with achiral proligands is stored in a file named `enumD3hsI-stsk.gap` (an arbitrary name), which is placed in a work directory (`c:/fujita0/fujita2017/D3hsI-GAP/calC-GAP/`, an arbitrary name). To execute this file by the GAP system [23], the first line commented out by the `#` symbol is copied and paste after the `gap>` prompt in the command prompt of the Windows operating system. For the purpose of using the GAP function `calcCoeffGen` for calculating CI-CFs, the file named `CICFgenCC.gapfunc` [25] is loaded by means of the function `Read`. The output is stored in the log file named `enumD3hsI-stsklog` (an arbitrary name), which contains the data for constructing Table 4 (the partitions

$[\check{\theta}]_1 - [\check{\theta}]_{11}$). For the purpose of calculating the data for Tables 5 (the partitions $[\check{\theta}]_{12} - [\check{\theta}]_{39}$), 6 (the partitions $[\check{\theta}]_{40} - [\check{\theta}]_{55}$), and 7 (the partitions $[\check{\theta}]_{56} - [\check{\theta}]_{66}$), the respective partitions are loaded in place of the partitions $[\check{\theta}]_1 - [\check{\theta}]_{11}$ shown in this source list.

```
#Read("c:/fujita0/fujita2017/D3hsI-GAP/calc-GAP/enumD3hsI-stsk.gap");
LogTo("c:/fujita0/fujita2017/D3hsI-GAP/calc-GAP/enumD3hsI-stsklog.txt");

Read("c:/fujita0/fujita2017/D3hsI-GAP/calc-GAP/CICFgenCC.gapfunc"); #Loading of CICFgenCC.gapfunc

D3 := Group([(1,2,3)(4,5,6), (1,4)(2,6)(3,5)]);
CICF_D3 := CalcConjClassCICF(D3, 6, 8);

D3h := Group([(2,3)(5,6)(7,8), (1,2)(4,5)(7,8), (1,4)(2,5)(3,6)(7,8)]);
CICF_D3h := CalcConjClassCICF(D3h, 6, 8);

D3hsI := Group([(7,8), (2,3)(5,6), (1,2)(4,5), (1,4)(2,5)(3,6)]);
CICF_D3hsI := CalcConjClassCICF(D3hsI, 6, 8);

cd3hsI := Group([(7,8), (3,6), (2,3)(5,6), (1,2)(4,5)]);
CICF_cd3hsI := CalcConjClassCICF(cd3hsI, 6, 8);

ccD3hsI := Group([(7,8), (5,6), (4,5), (3,4), (2,3), (1,2)]);
CICF_ccD3hsI := CalcConjClassCICF(ccD3hsI, 6, 8);

H := Indeterminate(Rationals, "H"); V := Indeterminate(Rationals, "V");
A := Indeterminate(Rationals, "A"); B := Indeterminate(Rationals, "B");
C := Indeterminate(Rationals, "C"); D := Indeterminate(Rationals, "D");
p := Indeterminate(Rationals, "p"); q := Indeterminate(Rationals, "q");
r := Indeterminate(Rationals, "r"); s := Indeterminate(Rationals, "s");
t := Indeterminate(Rationals, "t"); u := Indeterminate(Rationals, "u");

b_1 := Indeterminate(Rationals, "b_1"); b_2 := Indeterminate(Rationals, "b_2");
b_3 := Indeterminate(Rationals, "b_3"); b_4 := Indeterminate(Rationals, "b_4");
b_5 := Indeterminate(Rationals, "b_5"); b_6 := Indeterminate(Rationals, "b_6");
a_1 := Indeterminate(Rationals, "a_1"); a_2 := Indeterminate(Rationals, "a_2");
a_3 := Indeterminate(Rationals, "a_3"); a_4 := Indeterminate(Rationals, "a_4");
a_5 := Indeterminate(Rationals, "a_5"); a_6 := Indeterminate(Rationals, "a_6");
c_2 := Indeterminate(Rationals, "c_2"); c_4 := Indeterminate(Rationals, "c_4");
c_6 := Indeterminate(Rationals, "c_6");

aa_1 := H + A + B + C + D + V;
aa_2 := H^2 + A^2 + B^2 + C^2 + D^2 + V^2;
aa_3 := H^3 + A^3 + B^3 + C^3 + D^3 + V^3;
aa_4 := H^4 + A^4 + B^4 + C^4 + D^4 + V^4;
aa_5 := H^5 + A^5 + B^5 + C^5 + D^5 + V^5;
aa_6 := H^6 + A^6 + B^6 + C^6 + D^6 + V^6;
bb_1 := H + A + B + C + D + V + 2*(p + q + r + s + u + t);
bb_2 := H^2 + A^2 + B^2 + C^2 + D^2 + V^2 + 2*(p^2 + q^2 + r^2 + s^2 + t^2 + u^2);
bb_3 := H^3 + A^3 + B^3 + C^3 + D^3 + V^3 + 2*(p^3 + q^3 + r^3 + s^3 + t^3 + u^3);
bb_4 := H^4 + A^4 + B^4 + C^4 + D^4 + V^4 + 2*(p^4 + q^4 + r^4 + s^4 + t^4 + u^4);
bb_5 := H^5 + A^5 + B^5 + C^5 + D^5 + V^5 + 2*(p^5 + q^5 + r^5 + s^5 + t^5 + u^5);
bb_6 := H^6 + A^6 + B^6 + C^6 + D^6 + V^6 + 2*(p^6 + q^6 + r^6 + s^6 + t^6 + u^6);
cc_2 := H^2 + A^2 + B^2 + C^2 + D^2 + V^2 + 2*p^2 + 2*q^2 + 2*r^2 + 2*s^2 + 2*t^2 + 2*u^2;
cc_4 := H^4 + A^4 + B^4 + C^4 + D^4 + V^4 + 2*p^4 + 2*q^4 + 2*r^4 + 2*s^4 + 2*t^4 + 2*u^4;
cc_6 := H^6 + A^6 + B^6 + C^6 + D^6 + V^6 + 2*p^6 + 2*q^6 + 2*r^6 + 2*s^6 + 2*t^6 + 2*u^6;

aaa_1 := H + A + B + C + D + V + p + q + r + s + t + u;
aaa_2 := H^2 + A^2 + B^2 + C^2 + D^2 + V^2 + p^2 + q^2 + r^2 + s^2 + t^2 + u^2;
aaa_3 := H^3 + A^3 + B^3 + C^3 + D^3 + V^3 + p^3 + q^3 + r^3 + s^3 + t^3 + u^3;
aaa_4 := H^4 + A^4 + B^4 + C^4 + D^4 + V^4 + p^4 + q^4 + r^4 + s^4 + t^4 + u^4;
aaa_5 := H^5 + A^5 + B^5 + C^5 + D^5 + V^5 + p^5 + q^5 + r^5 + s^5 + t^5 + u^5;
aaa_6 := A^6 + B^6 + C^6 + D^6 + H^6 + V^6 + p^6 + q^6 + r^6 + s^6 + t^6 + u^6;
bbb_1 := H + A + B + C + D + V + p + q + r + s + t + u;
bbb_2 := H^2 + A^2 + B^2 + C^2 + D^2 + V^2 + p^2 + q^2 + r^2 + s^2 + t^2 + u^2;
bbb_3 := H^3 + A^3 + B^3 + C^3 + D^3 + V^3 + p^3 + q^3 + r^3 + s^3 + t^3 + u^3;
bbb_4 := H^4 + A^4 + B^4 + C^4 + D^4 + V^4 + p^4 + q^4 + r^4 + s^4 + t^4 + u^4;
bbb_5 := H^5 + A^5 + B^5 + C^5 + D^5 + V^5 + p^5 + q^5 + r^5 + s^5 + t^5 + u^5;
bbb_6 := H^6 + A^6 + B^6 + C^6 + D^6 + V^6 + p^6 + q^6 + r^6 + s^6 + t^6 + u^6;
ccc_2 := H^2 + A^2 + B^2 + C^2 + D^2 + V^2 + p^2 + q^2 + r^2 + s^2 + t^2 + u^2;
ccc_4 := H^4 + A^4 + B^4 + C^4 + D^4 + V^4 + p^4 + q^4 + r^4 + s^4 + t^4 + u^4;
ccc_6 := H^6 + A^6 + B^6 + C^6 + D^6 + V^6 + p^6 + q^6 + r^6 + s^6 + t^6 + u^6;
```

```
f_D3 := Value(CICF_D3,
[a_1, a_2, a_3, a_4, a_5, a_6, b_1, b_2, b_3, b_4, b_5, b_6, c_2, c_4, c_6],
[aa_1, aa_2, aa_3, aa_4, aa_5, aa_6, bb_1, bb_2, bb_3, bb_4, bb_5, bb_6, cc_2, cc_4, cc_6]);

f_D3h := Value(CICF_D3h,
[a_1, a_2, a_3, a_4, a_5, a_6, b_1, b_2, b_3, b_4, b_5, b_6, c_2, c_4, c_6],
[aa_1, aa_2, aa_3, aa_4, aa_5, aa_6, bb_1, bb_2, bb_3, bb_4, bb_5, bb_6, cc_2, cc_4, cc_6]);

f_D3hsI := Value(CICF_D3hsI,
[a_1, a_2, a_3, a_4, a_5, a_6, b_1, b_2, b_3, b_4, b_5, b_6, c_2, c_4, c_6],
[aa_1, aa_2, aa_3, aa_4, aa_5, aa_6, bb_1, bb_2, bb_3, bb_4, bb_5, bb_6, cc_2, cc_4, cc_6]);

f_cd3hsI := Value(CICF_cd3hsI,
[a_1, a_2, a_3, a_4, a_5, a_6, b_1, b_2, b_3, b_4, b_5, b_6, c_2, c_4, c_6],
[aaa_1, aaa_2, aaa_3, aaa_4, aaa_5, aaa_6, bbb_1, bbb_2, bbb_3, bbb_4, bbb_5, bbb_6,
ccc_2, ccc_4, ccc_6]);

f_ccD3hsI := Value(CICF_ccD3hsI,
[a_1, a_2, a_3, a_4, a_5, a_6, b_1, b_2, b_3, b_4, b_5, b_6, c_2, c_4, c_6],
[aaa_1, aaa_2, aaa_3, aaa_4, aaa_5, aaa_6, bbb_1, bbb_2, bbb_3, bbb_4, bbb_5, bbb_6,
ccc_2, ccc_4, ccc_6]);

list_partitions := [];
calcCoeffGenD3hsI := function(list_partitions)
local list_ligand_L, l_pp;
list_ligand_L := [H,A,B,C,D,V,p,q,r,s,t,u];
l_pp := list_partitions;
Print("$", l_pp, "$&u",
calcCoeffGen(f_D3, list_ligand_L, list_partitions), "&u",
calcCoeffGen(f_D3h, list_ligand_L, list_partitions), "&u",
calcCoeffGen(f_D3hsI, list_ligand_L, list_partitions), "&u",
calcCoeffGen(f_cd3hsI, list_ligand_L, list_partitions), "&u",
calcCoeffGen(f_ccD3hsI, list_ligand_L, list_partitions), "\n\\n\\n");
end;

#"Print A6";
calcCoeffGenD3hsI([6,0,0,0,0,0,0,0,0,0,0]);
#"Print A5";
calcCoeffGenD3hsI([5,1,0,0,0,0,0,0,0,0,0]);
#"Print A4";
calcCoeffGenD3hsI([4,2,0,0,0,0,0,0,0,0,0]);
calcCoeffGenD3hsI([4,1,1,0,0,0,0,0,0,0,0]);
#"Print A3";
calcCoeffGenD3hsI([3,3,0,0,0,0,0,0,0,0,0]);
calcCoeffGenD3hsI([3,2,1,0,0,0,0,0,0,0,0]);
calcCoeffGenD3hsI([3,1,1,1,0,0,0,0,0,0,0]);
#"Print A2";
calcCoeffGenD3hsI([2,2,2,0,0,0,0,0,0,0,0]);
calcCoeffGenD3hsI([2,2,1,1,0,0,0,0,0,0,0]);
calcCoeffGenD3hsI([2,1,1,1,1,0,0,0,0,0,0]);
#"Print A1";
calcCoeffGenD3hsI([1,1,1,1,1,1,0,0,0,0,0]);

LogTo();
```

References

- [1] I. Ugi, J. Dugundji, R. Kopp, D. Marquarding, *Perspectives in Theoretical Stereochemistry*, Springer, Heidelberg, 1984.
- [2] K. Mislow, J. Siegel, Stereoisomerism and local chirality, *J. Am. Chem. Soc.* **106** (1984) 3319–3328.
- [3] M. A. Armstrong, *Groups and Symmetry*, Springer, New York, 1988.
- [4] W. Ledermann, A. J. Weir, *Introduction to Group Theory*, Addison Wesley Longman, New York, 1996.
- [5] D. E. Cohen, *Combinatorial Group Theory: A Topological Approach*, Cambridge Univ. Press, Cambridge, 1989.
- [6] https://en.wikipedia.org/wiki/Dihedral_group.
- [7] S. Fujita, α, β -itemized enumeration of inositol derivatives and m -gonal homologs by extending Fujita's proligand method, *Bull. Chem. Soc. Jpn.* **90** (2017) 343–366.
- [8] S. Fujita, Chirality fittingness of an orbit governed by a coset representation. Integration of point-group and permutation-group theories to treat local chirality and prochirality, *J. Am. Chem. Soc.* **112** (1990) 3390–3397.
- [9] S. Fujita, *Symmetry and Combinatorial Enumeration in Chemistry*, Springer, Berlin, 1991.
- [10] S. Fujita, *Diagrammatical Approach to Molecular Symmetry and Enumeration of Stereoisomers*, Univ. Kragujevac, Kragujevac, 2007.
- [11] S. Fujita, Graphs to chemical structures 1. Sphericity indices of cycles for stereochemical extension of Pólya's theorem, *Theor. Chem. Acc.* **113** (2005) 73–79.
- [12] S. Fujita, Graphs to chemical structures 2. Extended sphericity indices of cycles for stereochemical extension of Pólya's coronas, *Theor. Chem. Acc.* **113** (2005) 80–86.
- [13] S. Fujita, Graphs to chemical structures 3. General theorems with the use of different sets of sphericity indices for combinatorial enumeration of nonrigid stereoisomers, *Theor. Chem. Acc.* **115** (2006) 37–53.
- [14] S. Fujita, *Combinatorial Enumeration of Graphs, Three-Dimensional Structures, and Chemical Compounds*, Univ. Kragujevac, Kragujevac, 2013.

- [15] S. Fujita, Combinatorial enumeration of cubane derivatives as three-dimensional entities. I. Gross enumeration by the proligand method, *MATCH Commun. Math. Comput. Chem.* **67** (2012) 5–24.
- [16] S. Fujita, Combinatorial enumeration of cubane derivatives as three-dimensional entities. II. Gross enumeration by the markaracter method, *MATCH Commun. Math. Comput. Chem.* **67** (2012) 25–54.
- [17] S. Fujita, Combinatorial enumeration of cubane derivatives as three-dimensional entities. III. Gross enumeration by the characteristic-monomial method, *MATCH Commun. Math. Comput. Chem.* **67** (2012) 649–668.
- [18] S. Fujita, Combinatorial enumeration of cubane derivatives as three-dimensional entities. IV. Gross enumeration by the extended superposition method, *MATCH Commun. Math. Comput. Chem.* **67** (2012) 669–686.
- [19] S. Fujita, Combinatorial enumeration of cubane derivatives as three-dimensional entities. V. Gross enumeration by the double coset representation method, *MATCH Commun. Math. Comput. Chem.* **67** (2012) 687–712.
- [20] S. Fujita, *Mathematical Stereochemistry*, De Gruyter, Berlin, 2015.
- [21] S. Fujita, Stereogenicity revisited. Proposal of holantimers for comprehending the relationship between stereogenicity and chirality, *J. Org. Chem.* **69** (2004) 3158–3165.
- [22] S. Fujita, Pseudoasymmetry, stereogenicity, and the *RS*-nomenclature comprehended by the concepts of holantimers and stereoisograms, *Tetrahedron* **60** (2004) 11629–11638.
- [23] <https://www.gap-system.org/>.
- [24] S. Fujita, Computer-oriented representations of point groups and cycle indices with chirality fittingness (CI-CFs) calculated by the GAP system. Enumeration of three-dimensional structures of ligancy 4 by Fujita’s proligand method, *MATCH Commun. Math. Comput. Chem.* **76** (2016) 379–400.
- [25] S. Fujita, Computer-oriented representations of O_h -skeletons for supporting combinatorial enumeration by Fujita’s proligand method. GAP calculation of cycle indices with chirality fittingness (CI-CFs), *MATCH Commun. Math. Comput. Chem.* **77** (2017) 409–442.
- [26] S. Fujita, Computer-oriented representations of *RS*-stereoisomeric groups and cycle indices with chirality fittingness (CI-CFs) calculated by the GAP system. Enumeration of *RS*-stereoisomers by Fujita’s proligand method, *MATCH Commun. Math. Comput. Chem.* **77** (2017) 443–478.

- [27] S. Fujita, Misleading classification of isomers and stereoisomers in organic chemistry, *Bull. Chem. Soc. Jpn.* **87** (2014) 1367–1378.
- [28] S. Fujita, Classification of stereoisomers. Flowcharts without and with the intermediate concept of *RS*-stereoisomers for mediating between enantiomers and stereoisomers, *Tetrahedron: Asymmetry* **27** (2016) 43–62.
- [29] G. Pólya, Kombinatorische Anzahlbestimmungen für Gruppen, Graphen und chemische Verbindungen, *Acta Math.* **68** (1937) 145–254.
- [30] G. Pólya, R. C. Read, *Combinatorial Enumeration of Groups, Graphs, and Chemical Compounds*, Springer, New York, 1987.